ELSEVIER

Detrital-zircon geochronology of Paleozoic sedimentary rocks in the Hangay–Hentey basin, north-central Mongolia: Implications for the tectonic evolution of the Mongol–Okhotsk Ocean in central Asia

Thomas K. Kelty [a,*], An Yin [b,c,d], Batulzii Dash [e], George E. Gehrels [f], Angela E. Ribeiro [a]

[a] Department of Geological Sciences, California State University at Long Beach, Long Beach, CA 90840-3902, United States
[b] Department of Earth and Space Sciences, University of California, Los Angeles, CA 90095-1567, United States
[c] Institute of Geophysics and Planetary Physics, University of California, Los Angeles, CA 90095-1567, United States
[d] Structural Geology Group, China University of Geosciences, Beijing, People's Republic of China
[e] Department of Geology, Mongolian University of Science and Technology, Ulaan Baatar 210646, Mongolia
[f] Department of Geosciences, University of Arizona, Tucson, Arizona 85721, United States

Abstract

Understanding the development of the Central Asian Orogenic System (CAOS), which is the largest Phanerozoic accretionary orogen in the world, is critical to the determination of continental growth mechanisms and geological history of central Asia. A key to unraveling its geological history is to ascertain the origin and tectonic setting of the large flysch complexes that dominate the CAOS. These complexes have been variably interpreted as deep-marine deposits that were accreted onto a long-evolving arc against large continents to form a mega-accretionary complex or sediments trapped in back-arc to fore-arc basins within oceanic island-arc systems far from continents. To differentiate the above models we conducted U–Pb geochronological analyses of detrital-zircon grains from turbidites in the composite Hangay–Hentey basin of central Mongolia. This basin was divided by a Cenozoic fault system into the western and eastern sub-basins: the Hangay Basin in the west and Hentey basin in the east. This study focuses on the Hentey basin and indicates two groups of samples within this basin: (1) a southern group that were deposited after the earliest Carboniferous (∼339 Ma to 354 Ma) and a northern group that were deposited after the Cambrian to Neoproterozoic (∼504 Ma to 605 Ma). The samples from the northern part of the basin consistently contain Paleoproterozoic and Archean zircon grains that may have been derived from the Tuva–Mongol massif and/or the Siberian craton. In contrast, samples from the southern part of the basin contain only a minor component of early Paleozoic to Neoproterozoic zircon grains, which were derived from the crystalline basement bounding the Hangay–Hentey basin. Integrating all the age results from this study, we suggest that the Hangay–Hentey basin was developed between an island-arc system with a Neoproterozoic basement in the south and an Andean continental-margin arc in the north. The initiation of the southern arc occurred at or after the early Carboniferous, allowing accumulation of a flysch complex in a long-evolving accretionary complex.
© 2007 Elsevier B.V. All rights reserved.

Keywords: Mongol–Okhotsk Ocean; Hangay–Hentey basin; Detrital-zircon geochronology; Central Asian Orogenic System; Central Asian Orogenic Belt

1. Introduction

The Central Asian Orogenic System (CAOS) or the Central Asian Orogenic Belt was a site of significant continental growth in the Phanerozoic (Zonenshain et al., 1990; Sengör et al., 1993;

Sengör and Natal'in, 1996; Jahn et al., 2004; Windley et al., 2007). Understanding its tectonic history has important implications for the growth mechanisms of continental crust in Earth's history (Kovelenko et al., 2004). The development of the CAOS has been attributed to the following competing processes: (1) progressive duplication of a long-evolving arc with its original length exceeding 5000 km, which was subsequently shortened in map view by syn-subduction and strike-

---

slip faulting between ~ 620 and 360 Ma (Sengör et al., 1993; Sengör and Natal'in, 1996), (2) collision of multiple island arcs with Siberia and China (Chen and Hsü, 1995; Badarch et al., 2002; Xiao et al., 2003, 2004a,b; Windley et al., 2007), and (3) collision of micro-continents rifted from Gondwanaland onto the Siberian craton (e.g., Dobretsov et al., 1996). Although these competing hypotheses have distinctive predictions regarding the paleogeographic and tectonic origins of individual
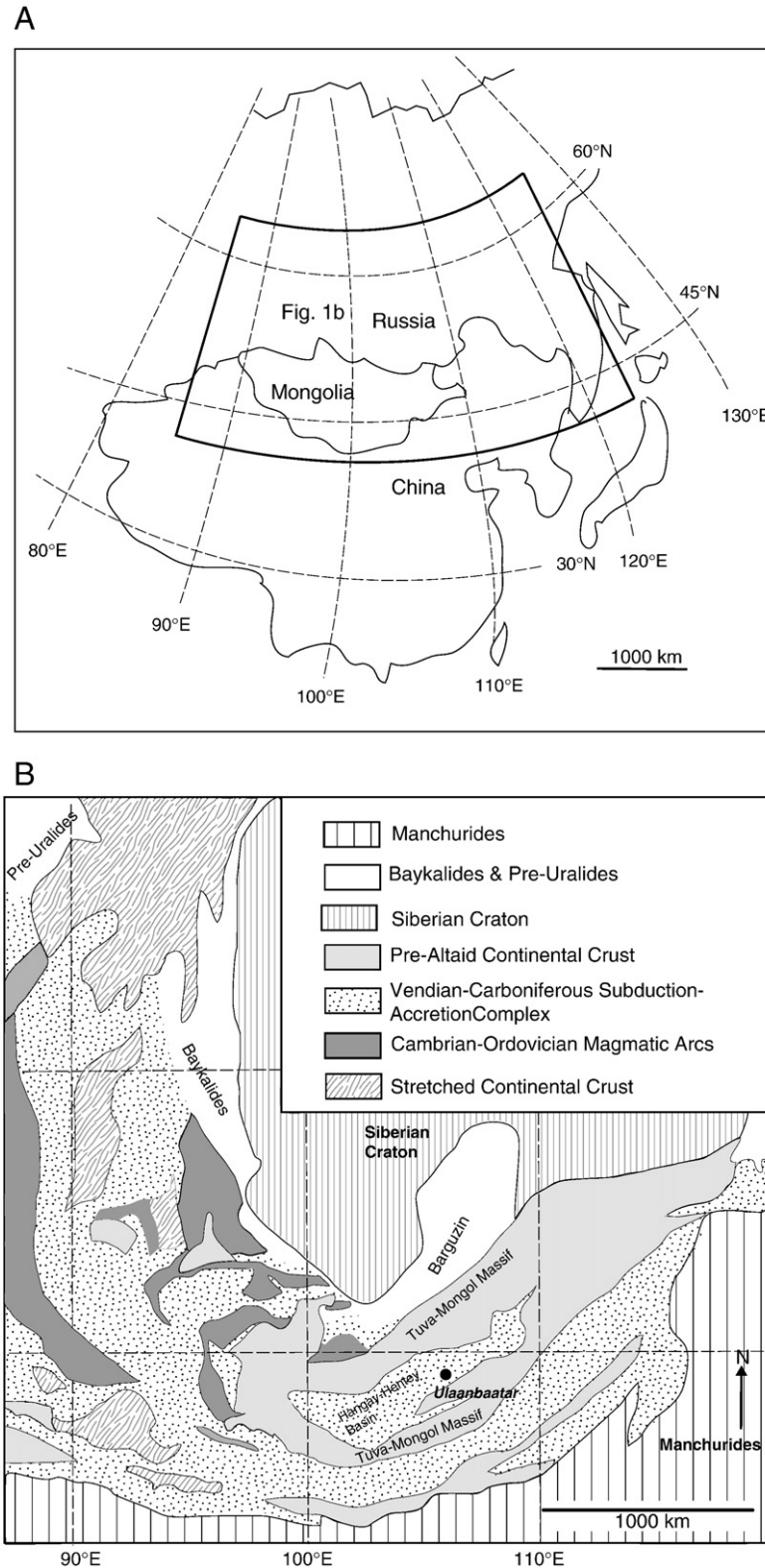

Fig. 1. Location (A) and tectonic (B) maps of the central part of the Central Asian Orogenic System, simplified from Sengör and Natal'in (1996).

terranes across the orogen, differentiating them has been a challenge. The low-grade flysch complexes dominate the orogen and their tectonic settings are poorly understood (e.g., Sengör et al., 1993; Badarch et al., 2002) (Fig. 1). The flysch complexes have been interpreted to represent large accretionary complexes fringing a long-evolving arc along continental margins (Sengör et al., 1993; Sengör and Natal'in, 1996). They have also been interpreted to represent back-arc/fore-arc basin deposits within arcs formed in an intra-oceanic setting (Badarch et al., 2002) or along continental margins (Hsü and Chen, 1999).

The above models on the origin of flysch basins in the CAOS have specific predictions about the provenance and age distribution of their sedimentary detritus. For example, the continental-margin-arc model predicts the basins to have received significant Precambrian sediments (Fig. 2A). In contrast, the intra-oceanic-arc model predicts that the flysch sediments were derived exclusively from a nearby arc (Fig. 2B).

Finally, the rifted-continental-arc model predicts the arc to be sandwiched by flysch basins (back-arc and fore-arc basins), all of which contain a significant Precambrian signature (Fig. 2C).

To test the above models we conducted U–Pb detrital-zircon geochronology on late Paleozoic meta-sedimentary rocks from the Hangay–Hentey basin in north-central Mongolia. Because this basin was the largest flysch basin in the CAOS and located at its core (Fig. 1), understanding its provenance, timing of deposition, and tectonic setting has important implications for testing the competing hypotheses with regard to the origin of the Hangay–Hentey basin and the overall evolution of the CAOS.
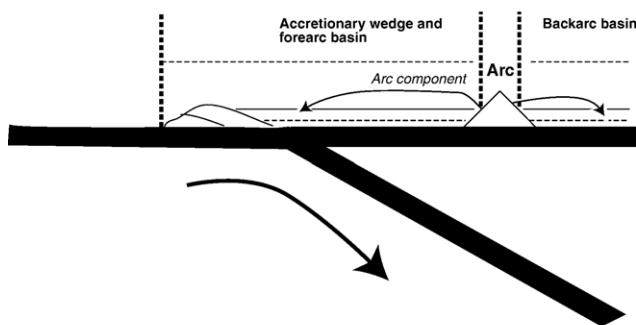
2. Regional geology

2.1. Hangay–Hentey Basin

The 200- to 300-km wide and 1000-km long Hangay–Hentey basin in central and eastern Mongolia was part of the
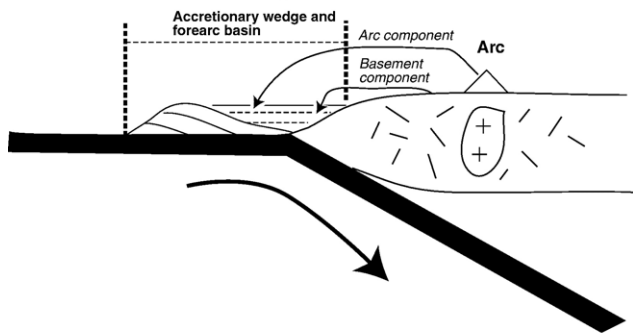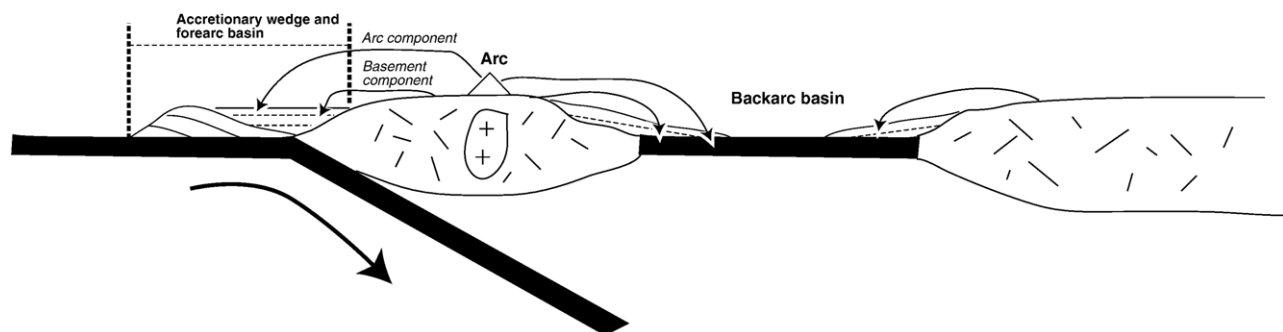

Fig. 2. Three end-member models for the formation of large flysch basins in the Central Asian Orogenic System. (A) Andean-type continental-margin-arc model. (B) Island-arc model. (C) Marginal arc rifted from nearby continent. See text for discussion.
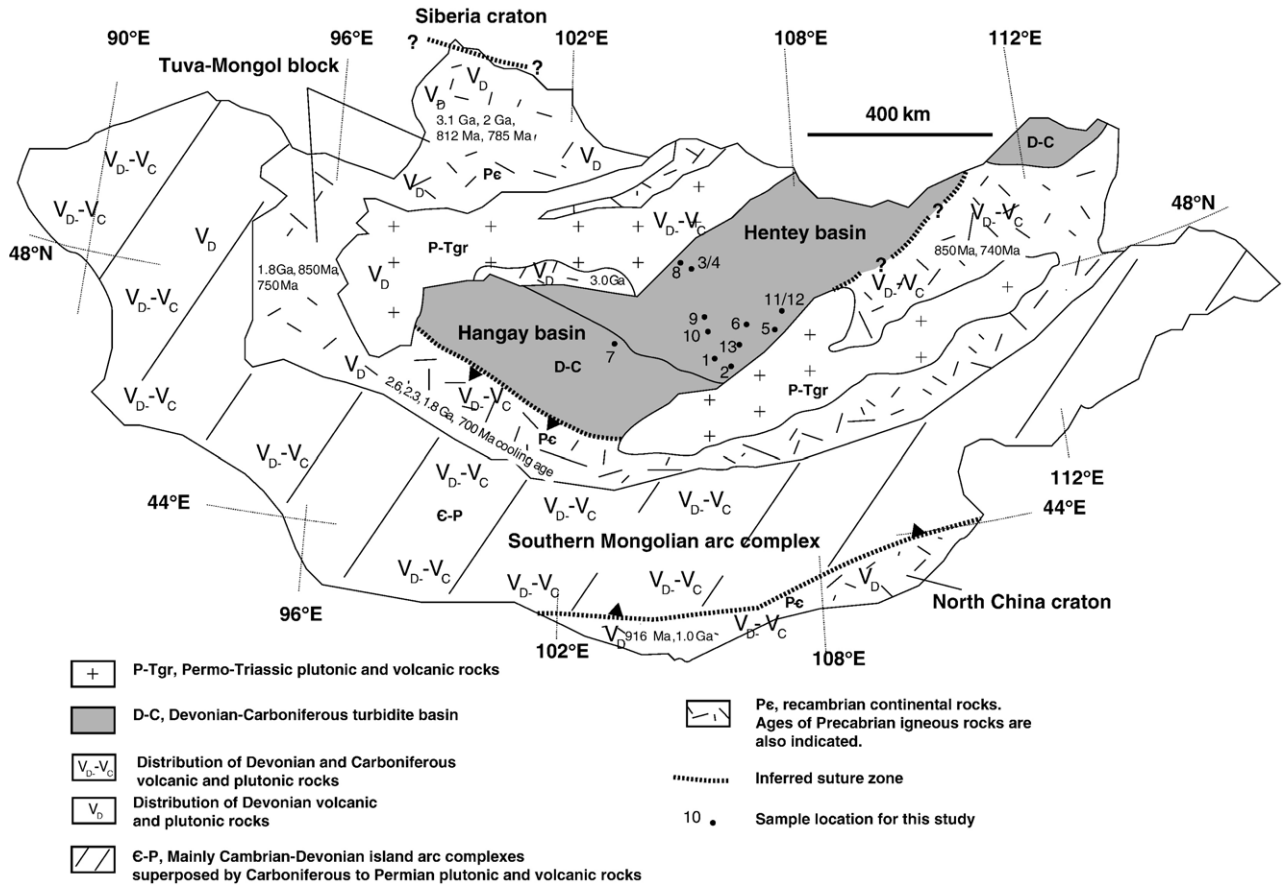
Fig. 3. Tectonic map of Mongolia, simplified from Badarch et al. (2002). Sample locations for this study and the major age provinces surrounding the Hangay–Hentey basin are also indicated. The V_D and V_D–V_C map symbols indicate the locations of Devonian and Devonian–Carboniferous igneous rocks, respectively. The Hangay–Hentey basin for this figure was defined from Sengör and Natal'in (1996) as a Vendian to Carboniferous subduction–accretion complex formed in the "Khangai–Khantey Ocean." Badarch et al. (2002) have a more spatially and time restricted definition of the Hangay–Hentey basin to be a Devonian to Carboniferous turbidite basin.

2500-km long Mongol–Okhotsk Ocean that extends from central Mongolia in the west to the Okhotsk Ocean in the east (Sengör and Natal'in, 1996; Yin and Nie, 1996) (Fig. 1). The western termination of the Mongol–Okhotsk Ocean was abrupt and its cause remains uncertain (see discussion on tectonic models below). The Hangay–Hentey basin has two sub-domains separated by a northwest-striking Cenozoic fault system: the Hangay basin in the west and the Hentey basin in the east (Fig. 3). The basin consists mainly of Devonian to Carboniferous turbidites that were folded and faulted and intruded or overlain by Mesozoic and Cenozoic igneous rocks (Tomurtogoo, 2006). The basement of the Devonian–Carboniferous turbidites was uncertain, as the contact between the sequence and the older rocks are tectonic (Badarch et al., 2002). Fragments of Ordovician and Silurian chert were tectonically mixed with Devonian and Carboniferous strata in the Hangay–Hentey basin (e.g., Kurihara et al., 2006). They were also in fault contact against a sequence of Ordovician strata along the northeastern margin of the basin (Badarch et al., 2002). Because the basin has been extensively intruded by Permian granites, Jahn et al. (2004) used geochemical tracers to suggest that the Hangay–Hentey basin was either floored by an enriched mantle or a Precambrian basement.

Although marine sedimentation ceased in the late Permian in the Hangay–Hentey basin, marking the closure of the Paleo-Asian ocean, the eastern segment of the Mongol–Okhotsk Ocean continued to receive marine sedimentation and its oceanic floor was subducting below North China until the Jurassic due to diachronous closure of this large and complex oceanic basin (Zorin et al., 1993; Yin and Nie, 1996; Halim et al., 1998).

2.2. Tuva–Mongol continental block

The Hangay–Hentey basin was sandwiched by the Precambrian Tuva–Mongol massif (also known as the central Mongolian massif) (Figs. 1 and 3). The massif forms a tight "V" in map view, opening towards the east (Sengör and Natal'in, 1996). The Tuva–Mongol massif was considered either as an isolated micro-continent in the Paleo-Asian ocean in the Late Proterozoic and Cambrian (Zorin et al., 1993; Mossakovsky et al., 1994; Zorin, 1999), a Precambrian continental strip connecting the much larger Siberian craton (Sengör and Natal'in, 1996), or a composite tectonic unit that was composed of several smaller continental blocks with uncertain tectonic relationships between each other (Badarch et al., 2002).
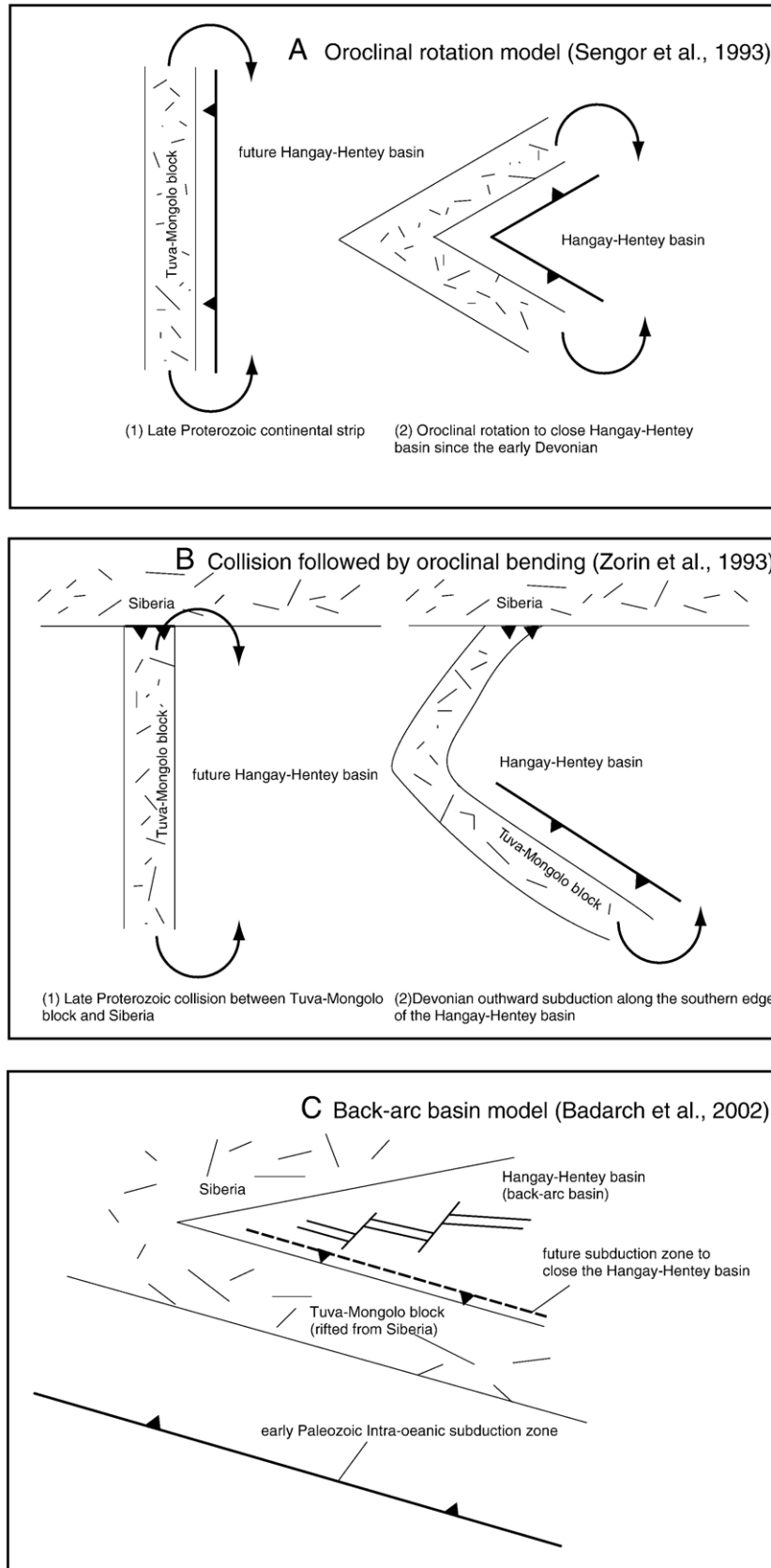
Fig. 4. Schematic diagrams showing models for the evolution of the Hangay–Hentey basin. (a) Model proposed by Sengör et al. (1993) and Sengör and Natal'in (1996) assumes the Tuva–Mongol massif was originally a linear belt that was later oroclinally folded for ~180° during the closure of the basin in the Devonian to the late Jurassic. (b) Model proposed by Zorin et al. (1993) requires that the Tuva–Mongol massif to have collided with Siberia in the late Proterozoic and was later rotated oroclinally for ~90° to close the Hangay–Hentey basin. (c) The back-arc basin model of Badarch et al. (2002) predicts limited (<40°) rotation of the Tuva–Mongol massif to close the Hangay–Hentey basin. See text for details of comparisons among the model predictions.

The northern arm of the Tuva–Mongol continental block was also divided by a large Permo-Triassic igneous province into the northern and southern parts (Fig. 3). South of the igneous province, the continental block consists of gneiss, migmatite, amphibolite, and schist, all intruded by anorthosite plutons (Badarch et al., 2002). The oldest anorthosite yields a ^{207}Pb/^{206}Pb age of ~3.0 Ga (Badarch et al., 2002). The metamorphosed basement was overlain by Neoproterozoic to early Cambrian limestone and volcanic rocks, and Devonian to early Carboniferous marine strata interbedded with andesite and rhyolite (Badarch et al., 2002). The above rock units were also intruded by Permian plutons. North of the igneous province, the northern arm of the continental block was exposed along the northernmost border of Mongolia (Fig. 3). This area exposes gneiss with Rb–Sr isochron age of ~3.1 Ga and U–Pb zircon age of ~2 Ga (Badarch et al., 2002). Archean and early Proterozoic metamorphic basement was thrust over by an island-arc complex that contains tonalitic plutons with ~812 Ma Rb–Sr isochron age and a U–Pb zircon age of ~785 Ma (Badarch et al., 2002).

Directly west of the Hangay–Hentey basin, the Tuva–Mongol continental block bends sharply (Fig. 3). Around the hinge zone area, the continental block was composed of a low-grade meta-volcanic complex with ~812 Ma felsic volcanic rocks (Badarch et al., 2002; Tomurtogoo, 2006). The complex was overlain by Neoproterozoic–early Cambrian marine strata and Devonian to Cretaceous non-marine volcanic and sedimentary rocks and was intruded by Devonian and Permian plutons (Badarch et al., 2002).

The southern arm of the Tuva–Mongol continental block was separated by a large Permian–Triassic igneous province (Fig. 3). In the west, the block was composed of Archean tonalitic gneiss (U–Pb zircon age of ~2650 Ma), granulite, amphibolite, minor quartzite, and 2.3-Ga and 1.8-Ga grano-dioritic dikes (Badarch et al., 2002; Tomurtogoo, 2006). The metamorphic basement was overlain by a Neoproterozoic meta-sedimentary sequence that yields a K–Ar muscovite cooling age of ~700 Ma (Fig. 3) (Badarch et al., 2002). This sequence, together with the basement, was overlain by Ordovician limestone, conglomerate, and sandstone, Silurian shale, Devonian to Permian volcanic rocks interlayered with marine strata,
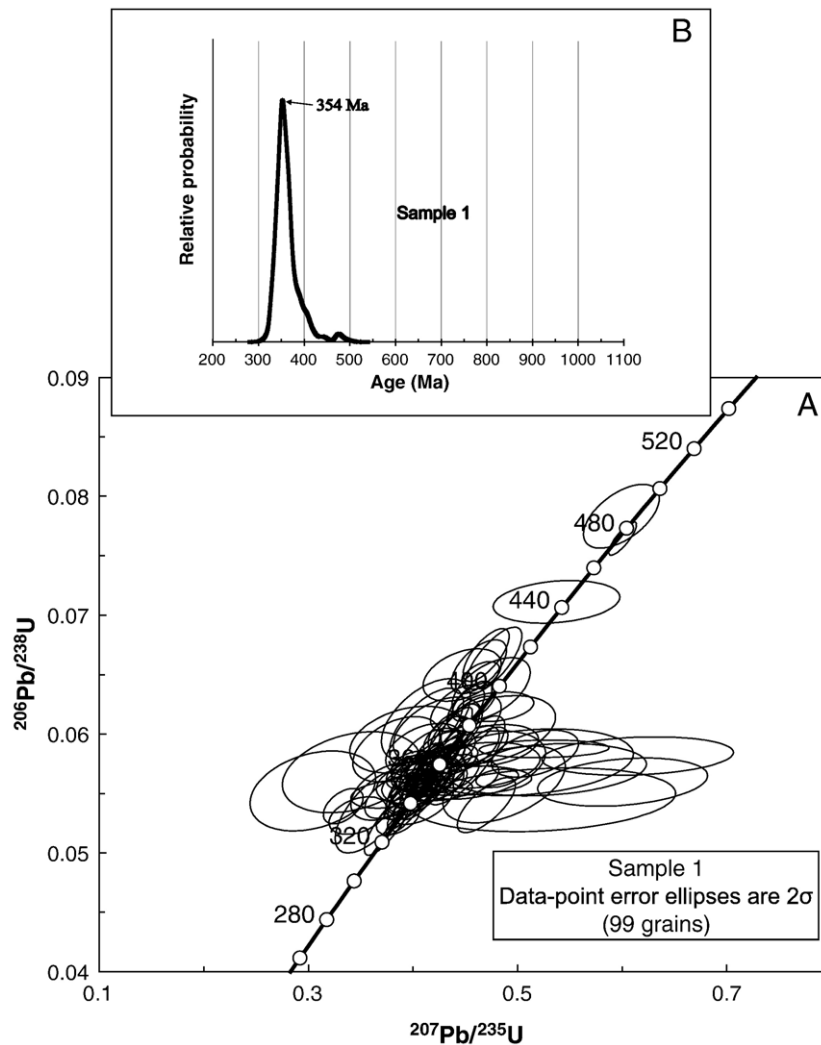

Fig. 5. (A) U–Pb concordia diagram of single detrital-zircon grains for Sample 1 (99 grains total). Error ellipses were at the 2σ level. (B) Relative-age-probability diagram for Sample 1. Note that the relative-age-probability curves show ages and uncertainties (plotted as a normal distribution about the age) from each sample.

and Jurassic–Cretaceous clastic sediments (Badarch et al., 2002). East of the Permo-Triassic igneous province, the northern arm of the Tuva–Mongol continental block was composed of Paleoproterozoic gneiss, amphibolite, schist, and marble, which were overlain by Neoproterozoic meta-sedimentary sequences (Badarch et al., 2002). The above rocks were intruded by plutons with a U–Pb zircon age of 740 Ma and Rb–Sr isochron age of 850 Ma (Badarch et al., 2002; Tomurtogoo, 2006). The Neoproterozoic sequence was overlain by Silurian marine sediments, Devonian volcanic rocks interbedded with carbonate and siliciclastic rocks, and Carboniferous volcanic rocks (Badarch et al., 2002; Tomurtogoo, 2006).

Directly south and west of the Tuva–Mongol microcontinental block was the vast southern Mongolia arc complex, comprised of diverse Paleozoic arc assemblages including island-arc complex, flysch basin deposits, ophiolitic fragments, and plutonic belts (Tomurtogoo, 2006). The island arcs were mostly developed in the Cambrian to Carboniferous (Badarch et al., 2002; Windley et al., 2007). This arc complex was bounded in the south by Precambrian continental rocks, which

may be continental fragments rifted from the North China craton (Fig. 3) (Badarch et al., 2002).

2.3. Devonian–Carboniferous arc magmatism

Devonian and Carboniferous arc assemblages surround the Hangay–Hentey basin. Devonian plutonism (alkaline granite and quartz syenite) was well developed ~100 km north of the Hangay–Hentey basin, between of the Selenga River and Lake Baikal (Wickham et al., 1995). Carboniferous to early Permian arc volcanism was mainly concentrated in Russia, northeast of the Selenga river, and in the southern Mongolian arc, which was south of the Hangay–Hentey basin (Fig. 3) (Wickham et al., 1995; Zorin, 1999; Badarch et al., 2002). Badarch et al. (2002) proposed that this pattern of arc magmatism implies that northward subduction may have ceased during the Devonian and the main arc development and the closure process of the Hangay–Hentey basin was probably accommodated by southward subduction of the basin below the southern arm of the Tuva–Mongol massif.
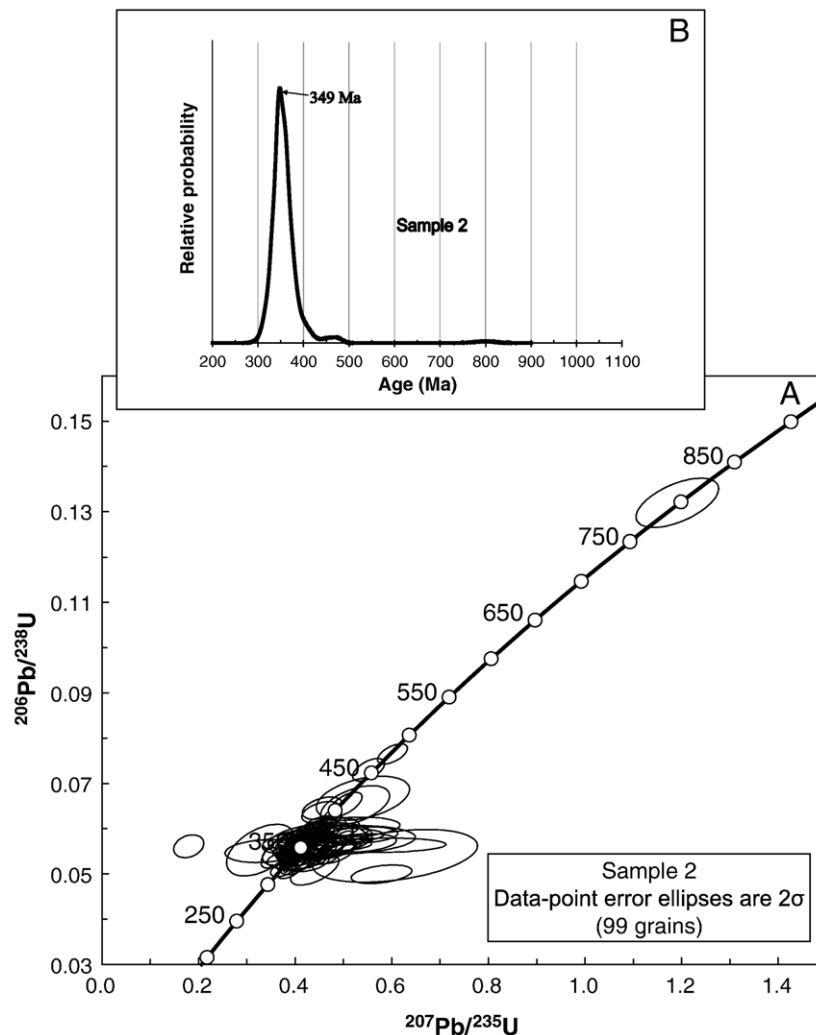

Fig. 6. (A) U–Pb concordia diagram of single detrital-zircon grains for Sample 2 (99 grains total). Error ellipses were at the 2σ level. (B) Relative-age-probability diagram for Sample 2. Note that the relative-age-probability curves show ages and uncertainties (plotted as a normal distribution about the age) from each sample.

2.4. Tectonic models for the development of the Hangay–Hentey Basin

The geological history of the Hangay–Hentey basin was linked with the evolution of the Mongol–Okhotsk Ocean. The timing of the ocean closure has been debated. Based on the last appearance of marine sedimentation, the closure of the Mongol–Okhotsk Ocean has been variably assigned to the early and middle Jurassic (Zorin et al., 1993; Didenko et al., 1994; Zorin, 1999) and late Jurassic (Jishun and Tingyu, 1989). However, the paleomagnetic arguments led Enkin et al. (1992) and Halim et al. (1998) to suggest that the closure of the Mongol–Okhotsk Ocean occurred in the late Jurassic and the continuous convergence between North China and Siberia continued until the late Cretaceous. In contrast to the above view that the Mongol–Okhotsk Ocean was synchronously closed, Nie et al. (1990), Nie (1991), and Yin and Nie (1993, 1996) suggested that the closure of the Mongol–Okhotsk Ocean was diachronous and occurred in the early Permian at its western termination in central Mongolia and in the latest Jurassic at its eastern termination in the Russian Far East near the Sea of Okhotsk.

The kinematic processes for the origin and final closure of the Mongol–Okhotsk Ocean and, thus, the Hangay–Hentey basin have also been debated. Three major hypotheses have been proposed. The first model, proposed by Sengör and Natal'in (1996), requires that the Precambrian Tuva–Mongol massif currently surrounding the Hangay–Hentey basin was a long linear strip connected with Siberia in the late Proterozoic (Fig. 4A). A subduction zone that dipped towards the continental strip was later oroclinally folded together with the continental strip sometime between the Devonian and the Jurassic. The oroclinal bending finally led to the closure of the Mongol–Okhotsk Ocean, where the Hangay–Hentey basin occupies its western segment. Sengör and Natal'in's (1996) model predicts that the Hangay–Hentey basin was a large oceanic basin with a history spanning from the late Proterozoic to the Jurassic. Because the same continental strip bounds the basin along its margin, it implies a similar provenance for Devonian to Carboniferous sediments that were derived from both sides of the basin (Fig. 4A). Structurally, the Sengör and Natal'in's (1996) model predict that the Devonian–Carboniferous turbidites were part of a large accretionary prism that
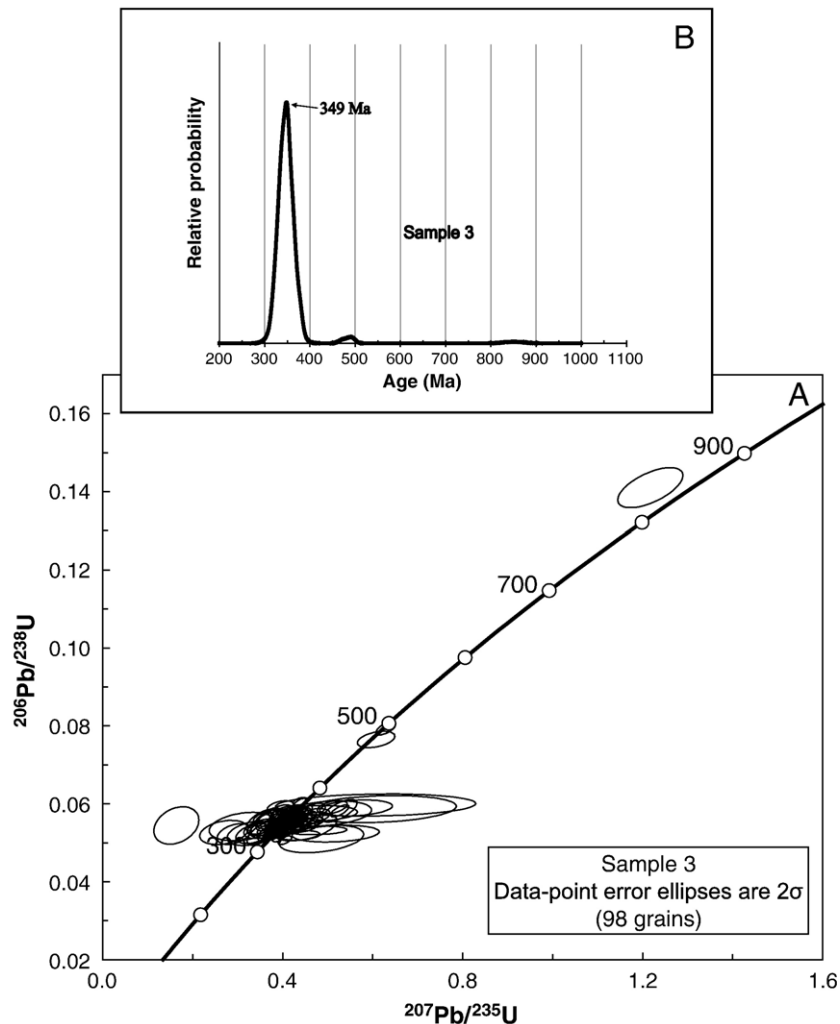

Fig. 7. (A) U–Pb concordia diagram of single detrital-zircon grains for Sample 3 (98 grains total). Error ellipses were at the 2σ level. (B) Relative-age-probability diagram for Sample 3. Note that the relative-age-probability curves show ages and uncertainties (plotted as a normal distribution about the age) from each sample.

began to develop in the late Proterozoic. The model also predicts a subduction zone that bounds both the north and south sides of the Hangay–Hentey basin (Fig. 4A).

The second model for the development of the Hangay–Hentey basin was suggested by Zorin et al. (1993). In their model, the Hangay–Hentey basin was formed as a remnant basin after the Tuva–Mongol micro-continent collided with Siberia in the late Proterozoic (Fig. 4B). This model implies that the basin originated as an embayment between a landmass (Siberia) and a thin continental strip (Tuva–Mongol massif). To close the basin, the model requires ∼90° of rotation of the Tuva–Mongol massif with respect to the Siberia craton. This model predicts that the closure of the Hangay–Hentey basin was accomplished by southward subduction along the southern margin of the basin, where the northern margin of the basin was a continuation of the Siberia craton.

The last major model for the development of the Hangay–Hentey basin was put forward by Badarch et al. (2002). These authors propose that the basin originated in a back-arc setting as a continental strip and was partially rifted away from Siberia (also see Xiao et al., 2003) (Fig. 4C). In this model, the Hangay–

Hentey basin was much like the Japan Sea with its northern and southern edges bounded by continuous, continental crust. This model predicts the presence of a north-dipping subduction zone and a south-dipping subduction zone below the southern arm of the Tuva–Mongol massif. In order to generate a back-arc basin, the southern subduction must have initiated earlier than the northern subduction which serves to close the basin. This model also requires relative rotation between Siberia and the southern arm of the Tuva–Mongol massif of less than 40°.

3. U–PB detrital-zircon geochronology

In order to determine the tectonic origin of the Hangay–Hentey basin and its relationship to its surrounding tectonic domains, we analyzed a total of 13 samples. Twelve of the 13 samples were located in the Hentey basin and one sample was from the easternmost Hangay basin (Fig. 3). All samples are medium-grained meta-sandstone. The age assignment of the meta-sedimentary units follows that of Badarch et al. (2002) and Tomurtogoo (2006) and range from Cambrian to Carboniferous. The exact age assignment of turbidite units in the existing
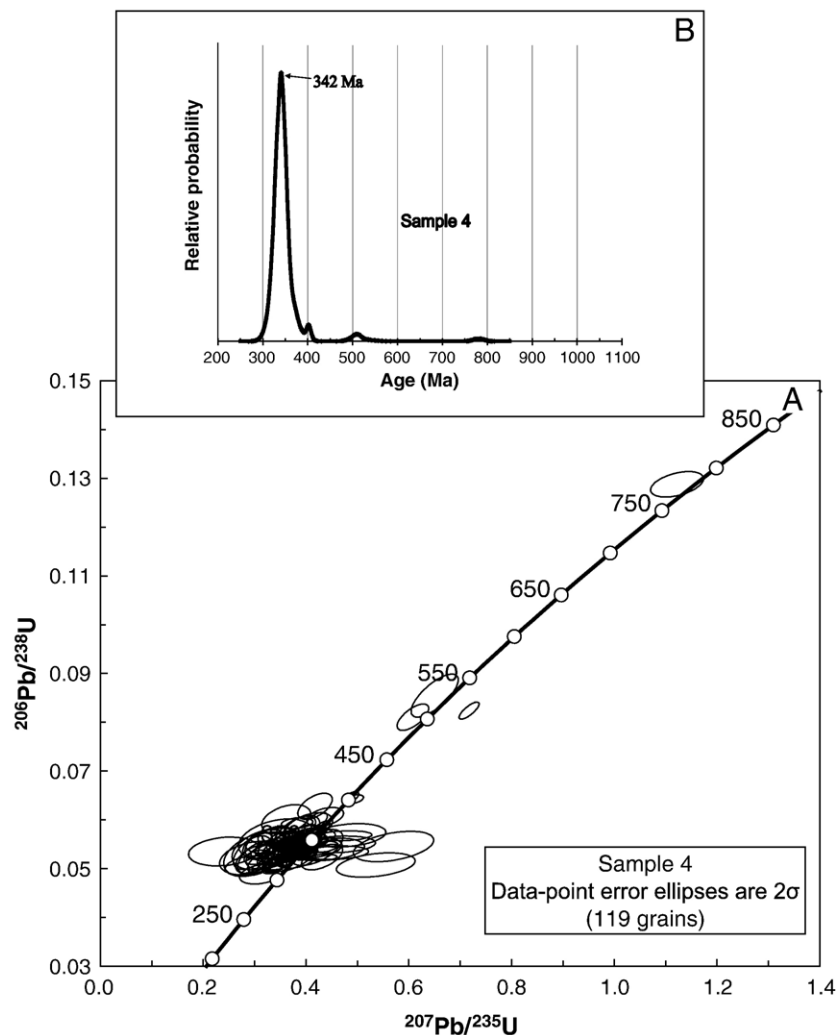

Fig. 8. (A) U–Pb concordia diagram of single detrital-zircon grains for Sample 4 (119 grains total). Error ellipses were at the 2σ level. (B) Relative-age-probability diagram for Sample 4. Note that the relative-age-probability curves show ages and uncertainties (plotted as a normal distribution about the age) from each sample.

literature was often vague and covers a wide range of >100 Ma (e.g., Dorjsuren et al., 2004; Tomurtogoo, 2006). This was because strata (1) were commonly folded such that their original stratigraphic relationships were difficult to reconstruct and (2) with diverse ages were commonly juxtaposed against one another in a small region (e.g., Kurihara et al., 2006). Because of these problems, the age assignment of Hangay–Hentey turbidite units was generally broad.

3.1. Method

Each sample was collected from a single outcrop (~4 kg). After mechanically crushing the samples, zircon grains were separated using magnetic and heavy liquid techniques. All zircon grains were set in epoxy and mounted adjacent to reference standard crystals. For each sample, approximately 100 zircon grains were randomly chosen to be ablated by a laser. U–Pb geochronology was performed on these grains using a multi-collector inductively coupled plasma mass spectrometry (LA-MC-ICPMS) at the Arizona LaserChron Center. The analyses involved ablation of zircon with a New Wave DUV193 Excimer laser (operating at a wavelength of 193 nm) using a spot diameter of 15 to 35 µm. The ablated material was carried in helium into the plasma source of a GVI Isoprobe, which was equipped with a flight tube of sufficient width that U, Th, and Pb isotopes were measured simultaneously. All measurements were made in static mode, using Faraday detectors for ^{238}U, ^{232}Th, $^{208-206}$Pb, and an ion-counting channel for ^{204}Pb. Ion yields are ~1.0 mv per ppm. Each analysis consists of one 20-second integration on peaks with the laser off (for backgrounds), 20 one-second integrations with the laser firing, and a 30 second delay to purge the previous sample and prepare for the next analysis. The ablation pit was ~15 µm in depth.

For each analysis, the measurement uncertainty in determining ^{206}Pb/^{238}U and ^{206}Pb/^{204}Pb is ~1–2% (2σ) in the ^{206}Pb/^{238}U age. The measurement uncertainties of ^{206}Pb/^{207}Pb and ^{206}Pb/^{204}Pb is ~1–2% (2σ) for ages that were >1.0 Ga, but were substantially larger for younger grains due to low intensity of the ^{207}Pb signal. For most analyses, the cross-over in precision of ^{206}Pb/^{238}U and ^{206}Pb/^{207}Pb ages occurs at 0.8–1.0 Ga.
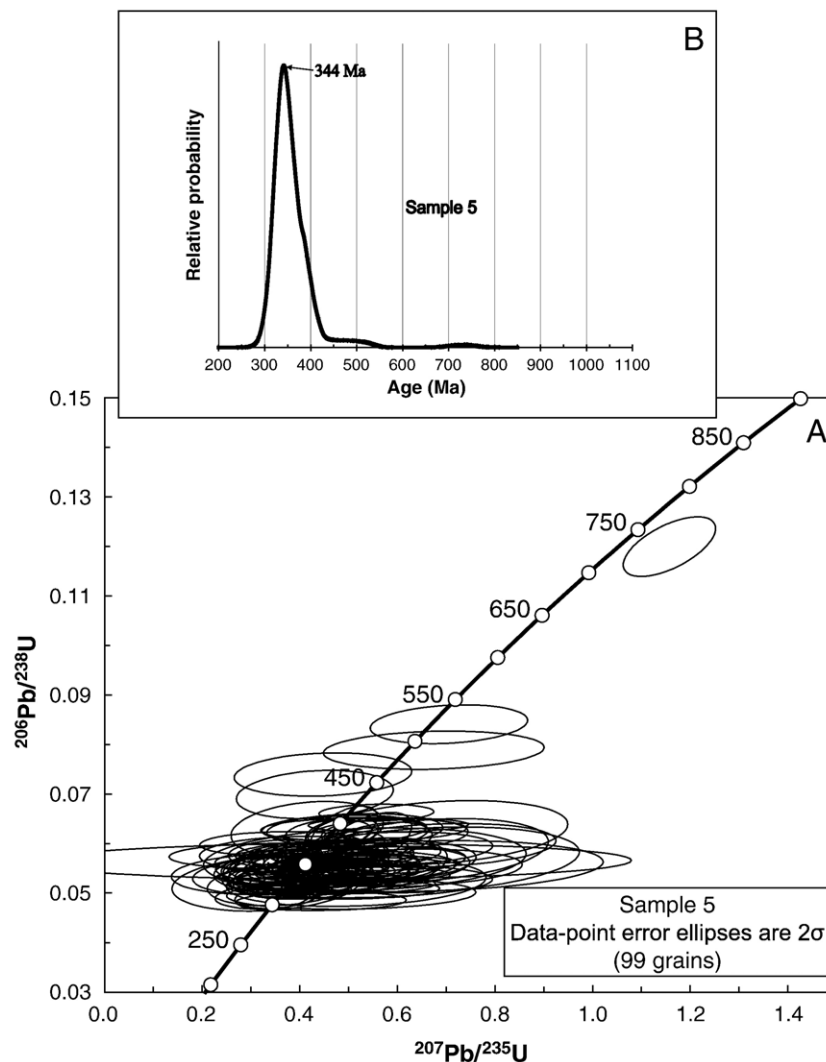

Fig. 9. (A) U–Pb concordia diagram of single detrital-zircon grains for Sample 5 (99 grains total). Error ellipses were at the 2σ level. (B) Relative-age-probability diagram for Sample 5. Note that the relative-age-probability curves show ages and uncertainties (plotted as a normal distribution about the age) from each sample.

Common Pb correction was accomplished by using the measured ^{204}Pb and assuming an initial Pb composition from Stacey and Kramers (1975) (with uncertainties of 1.0 for ^{206}Pb/^{204}Pb and 0.3 for ^{207}Pb/^{204}Pb). Our measurement of ^{204}Pb was unaffected by the presence of ^{204}Hg because backgrounds were measured on peaks (thereby subtracting any background ^{204}Hg and ^{204}Pb) and because very little Hg was present in the argon gas.

Inter-element fractionation of Pb/U is generally ∼ 20%, whereas fractionation of Pb isotopes was generally ∼ 2%. In-run analysis of fragments of a large zircon crystal (generally every fifth measurement) with known age of 564±4 Ma (2σ) was used to correct for this fractionation. The uncertainty resulting from the calibration correction was generally 1–2% (2σ) for both ^{206}Pb/^{207}Pb and ^{206}Pb/^{238}U ages.

The analytical data were reported in Table 1 (Supplementary material; Gehrels et al., 2006). Uncertainties shown in these tables are at the 1-sigma level and include only measurement uncertainties. Interpreted ages were based on ^{206}Pb/^{238}U for <800 Ma grains and on ^{206}Pb/^{207}Pb for >800 Ma grains. This

division at 800 Ma results from the increasing uncertainty of ^{206}Pb/^{238}U ages and the decreasing uncertainty of ^{206}Pb/^{207}Pb ages as a function of age. Analyses that are >30% discordant (by comparison of ^{206}Pb/^{238}U and ^{206}Pb/^{207}Pb ages) or >5% reverse discordant were not considered further. The resulting interpreted ages were shown on relative age-probability diagrams (from Ludwig, 2003). These diagrams show each age and its uncertainty (for measurement uncertainty only) as a normal distribution and sum all ages from a sample into a single curve.

3.2. Results

Sample 1 (47° 20.1′N, 105° 23.9′E) was collected from a turbidite sequence assigned to be a Silurian to Carboniferous age (Tomurtogoo, 2006) in the southernmost part of the Hentey basin (Fig. 3). The sequence was mainly meta-lithic-arkose, thinly bedded (<10 mm) with fining-upward ripple lamination. A total of 99 detrital-zircon grains were analyzed for U–Pb age determination and yielded an age range from ∼329 Ma to 486 Ma, with the main peak at around 354 Ma (Fig. 5A,B). This
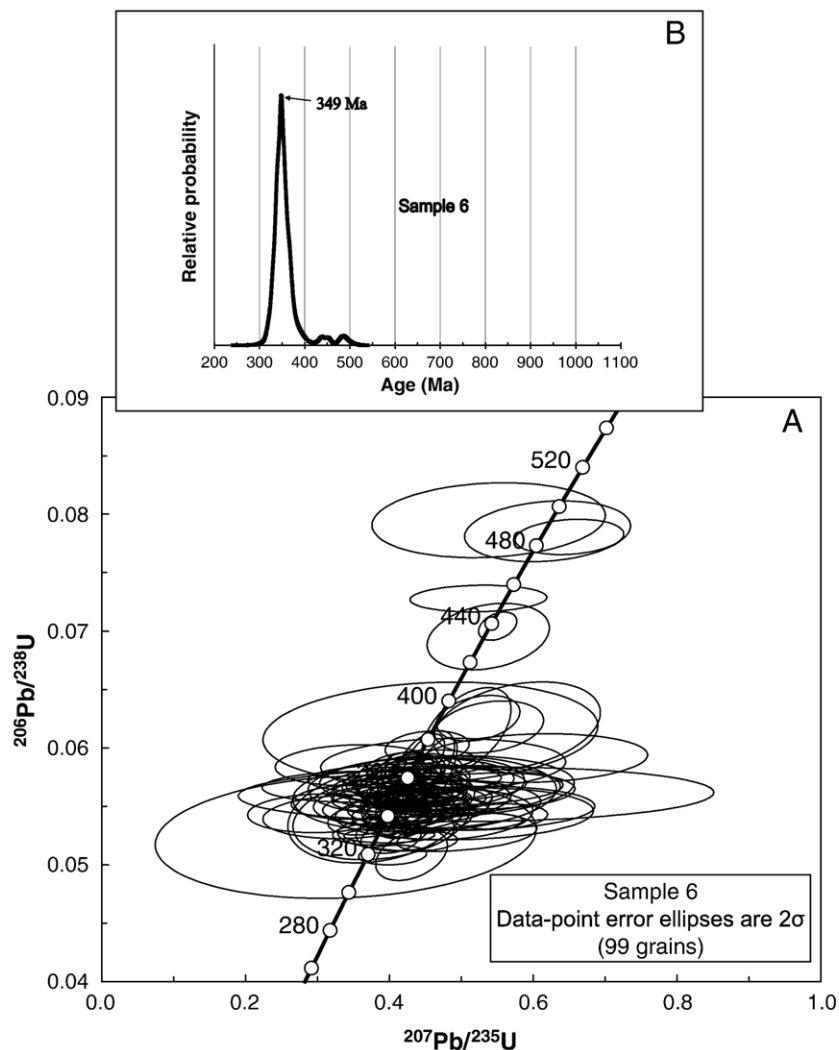

Fig. 10. (A) U–Pb concordia diagram of single detrital-zircon grains for Sample 6 (99 grains total). Error ellipses were at the 2σ level. (B) Relative-age-probability diagram for Sample 6. Note that the relative-age-probability curves show ages and uncertainties (plotted as a normal distribution about the age) from each sample.

sample contained three pre-Devonian zircon grains that were Ordovician in age. The 354-Ma peak age of zircon grains suggests that the depositional age of these meta-sediments must be younger than the earliest Carboniferous.

Sample 2 (47° 17.3′N, 105° 36.8′E) was collected from Silurian to Carboniferous age (Tomurtogoo, 2006) strata ~12 km southeast of Sample 1 (Fig. 3). These strata consist of thinly bedded, meta-lithic-arkose and meta-pelite and exhibits fining-upward sequence and erosional bases. Soft-sediment intraformational folding was commonly visible in the sequence, indicating rapid sedimentation on a slope and possible influence of tectonic activity. At this locality, these rocks were within a footwall of a north-dipping thrust that carries a radiolarian chert sequence in the hanging wall. A total of 99 zircon grains were analyzed for U–Pb age determination and yielded an age range from ~314 Ma to 799 Ma, with the main peak clustered at around 349 Ma (Fig. 6A,B). This sample contained three pre-Devonian zircon grains, two of which were Ordovician and one that was Neoproterozoic in age. The 349-Ma peak age of zircon grains suggests that the deposition of these rocks must be younger than the earliest Carboniferous.

Sample 3 (48° 16.4′N, 104° 41.6′E) was collected from a Silurian to Carboniferous age (Tomurtogoo, 2006) meta-lithic-arkose bed (Fig. 3), located in the northernmost part of the Hentey basin. A total of 98 grains were analyzed for this sample. The U–Pb zircon ages were between ~319 Ma and 851 Ma, with a peak at around 349 Ma. A few older grains were also detected from the sample: two of them with Ordovician ages and one with a Neoproterozoic age (851 Ma) (Fig. 7A,B). The 349-Ma peak age of zircon grains suggests that the depositional age of the strata was younger than the earliest Carboniferous.

Sample 4 (48° 15.3′N, 104° 38.8′E) was collected from a Silurian to Carboniferous age (Tomurtogoo, 2006) meta-lithic-arkose located ~10 km southwest of Sample 3 along the northern margin of the Hentey basin (Fig. 3). A total of 119 zircon grains were analyzed and were age dated between 308 and 781 Ma, with a peak at around 342 Ma (Fig. 8A,B). This sample contained four pre-Devonian zircon grains, three of which were Cambrian and one of which was Neoproterozoic in age (781 Ma). The 342-Ma peak age of zircon grains suggests that the depositional age of the strata must be younger than the earliest Carboniferous.
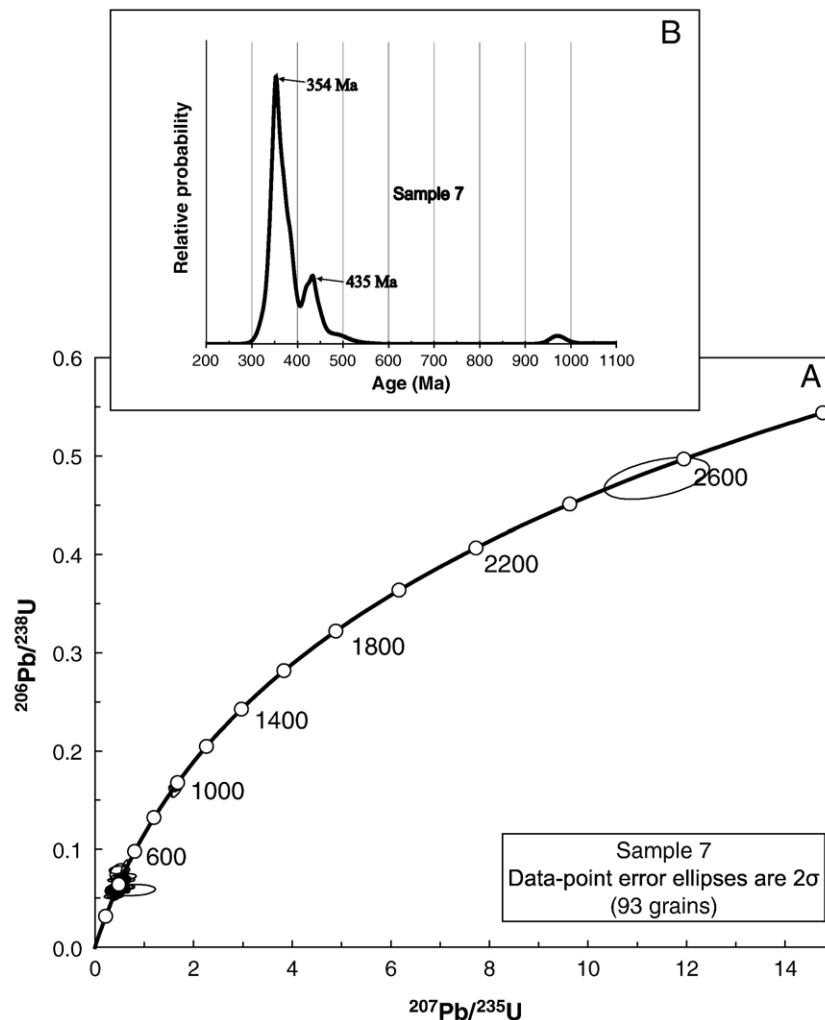

Fig. 11. (A) U–Pb concordia diagram of single detrital-zircon grains for Sample 7 (93 grains total). Error ellipses were at the 2σ level. (B) Relative-age-probability diagram for Sample 7. Note that the relative-age-probability curves show ages and uncertainties (plotted as a normal distribution about the age) from each sample.

Sample 5 (47° 24.9′N, 106° 44.0′E) was collected from a sequence of thinly bedded Silurian to Carboniferous age (Tomurtogoo, 2006) meta-lithic-arkose in the southern Hentey basin. It was located ~200 km east of Samples 1 and 2 (Fig. 3). The section where the sample was collected lies conformably below a 20-m-thick section of thinly bedded red chert. This relationship suggests a deep-water, open ocean origin for the sequence. A total of 99 zircon grains were analyzed. The ages were between 305 Ma and 730 Ma, with a peak around 344 Ma (Fig. 9A,B). This sample contained five pre-Devonian zircon grains. There were three of Silurian, Cambrian, and Neoproterozoic ages, respectively, and two zircon grains that were Ordovician age. The 344-Ma peak age of zircon grains suggests that deposition of the sediments occurred after the earliest Carboniferous.

Sample 6 (47° 52.6′N, 106° 37.1′E) was collected from a Silurian to Carboniferous age (Tomurtogoo, 2006) meta-lithic-arkose and meta-pelite sequence in the southern Hentey basin ~20 km west of Sample 5 (Fig. 3). A total of 99 zircon grains were analyzed for this sample and the ages range from

~320 Ma to 493 Ma, mostly clustering around the peak at 349 Ma (Fig. 10A,B). This sample contained six pre-Devonian zircon grains, two of which were Silurian, three of which were Ordovician and one of which was Cambrian age. The 349-Ma peak age of zircon grains suggest the deposition of the rocks occurred after the earliest Carboniferous.

Sample 7 (47° 17.8′N, 102° 30.0′E) was collected from an isoclinally folded sequence of Silurian to Carboniferous age (Tomurtogoo, 2006) meta-lithic-arkose in the easternmost edge of the Hangay basin (Fig. 3). This was the only sample analyzed from the Hangay basin and was included as a preliminary comparison to the samples collected in the Hentey basin (Fig. 3). A total of 93 zircon grains were measured for this sample with age results mostly between ~325 Ma and 2568 Ma, with a peak at ~354 Ma (Fig. 11A,B). There were also 20 grains with age results between ~417 Ma and 506 Ma, with a peak at ~435 Ma (Silurian). Four older grains at 967 Ma, 977 Ma, 1072 Ma, and 2589 Ma were also detected in the analysis. The clustered younger ages were similar to those in all other previously mentioned samples. However, the ages of the
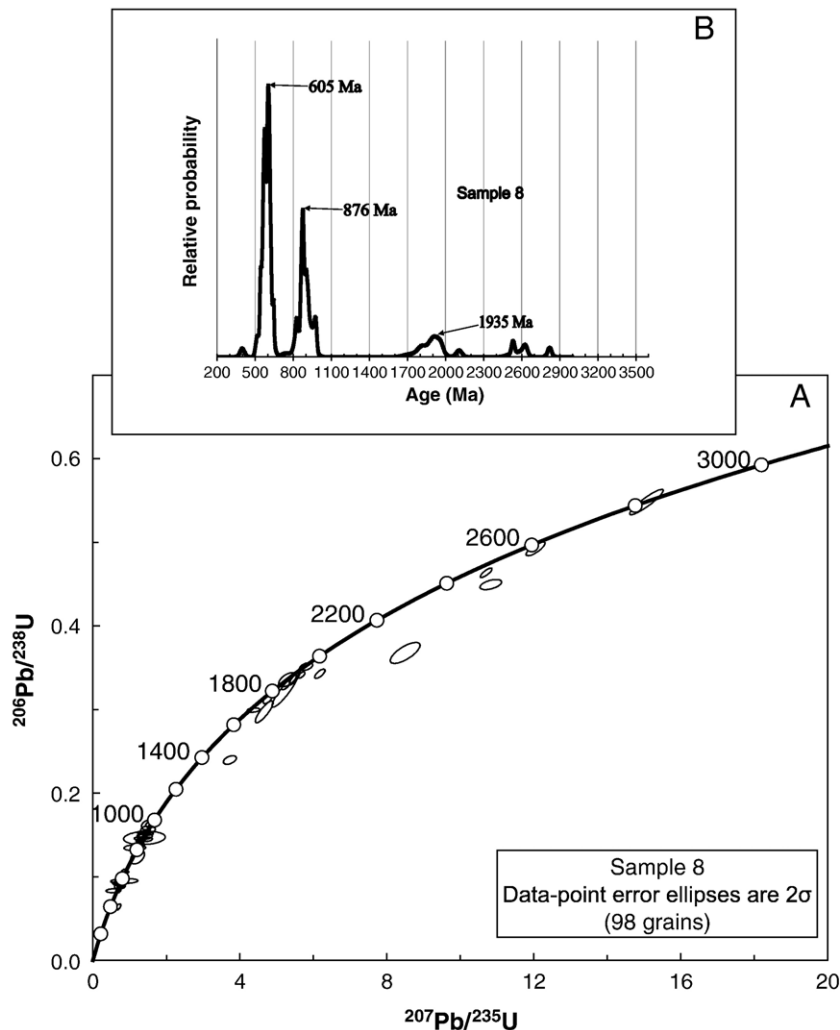

Fig. 12. (A) U–Pb concordia diagram of single detrital-zircon grains for Sample 8 (98 grains total). Error ellipses were at the 2σ level. (B) Relative-age-probability diagram for Sample 8. Note that the relative-age-probability curves show ages and uncertainties (plotted as a normal distribution about the age) from each sample.

four older grains were much older than other samples assigned to the Silurian to Carboniferous, particularly with the presence of an Archean age zircon grain. The 354-Ma peak age of zircon grains suggest that the strata from which the sample was collected were deposited after the earliest Carboniferous.

Sample 8 (48° 15.1′N, 104° 13.6′E) was collected from a meta-arenite bed in Cambrian–Ordovician (Tomurtogoo, 2006) strata along the northern most edge of the Hentey basin (Fig. 3). A total of 98 grains were measured which exhibited three Proterozoic age groups centered at 605 Ma, 876 Ma, and 1935 Ma. Five ages of zircon grains are Archean and range from ∼2532 Ma to 2821 Ma (Fig. 12A,B). The strongest age signals are at 612 Ma and 876 Ma and the rest were minor peaks. Also, an age of ∼399 Ma was also obtained from a single grain. The crystallization ages of the zircon grains suggest that the strata from which Sample 8 was collected were deposited after the Neoproterozoic. The single zircon grain that has an age of ∼399 Ma was not included in this interpretation of depositional age.

Sample 9 (47° 52.1′N, 105° 14.5′E) was a meta-lithic-arkose from a Cambrian–Ordovician (Tomurtogoo, 2006) sequence in the central part of the Hentey basin (Fig. 3). A total of 89 zircon grains were analyzed and yielded five major age groups at around 512 Ma, 584 Ma, 876 Ma, 1848 Ma and 2568 Ma. The youngest age revealed by the analysis was ∼483 Ma and the oldest age was at ∼3500 Ma (Fig. 13A,B). The presence of the youngest peak at ∼512 Ma suggests that the meta-sediments were deposited after the lower Cambrian.

Sample 10 (48° 14.4′N, 104° 18.4′E) was collected from an Ordovician–Silurian (Tomurtogoo, 2006) meta-lithic-arkose in the central part of the Hentey basin (Fig. 3). The meta-lithic-arkose was interlayered with radiolarian chert and conglomerate beds. The clasts of the conglomerate were dominantly chert and meta-sandstone. A total of 97 grains from this sample were analyzed and yielded an age distribution ranging from ∼451 Ma to 2849 Ma. Our analysis also revealed age peaks centered at 504 Ma, 572 Ma, 804 Ma, 901 Ma, 1811 Ma, 2418 Ma, and 2614 Ma (Fig. 14A,B). Similar to Sample 9, the
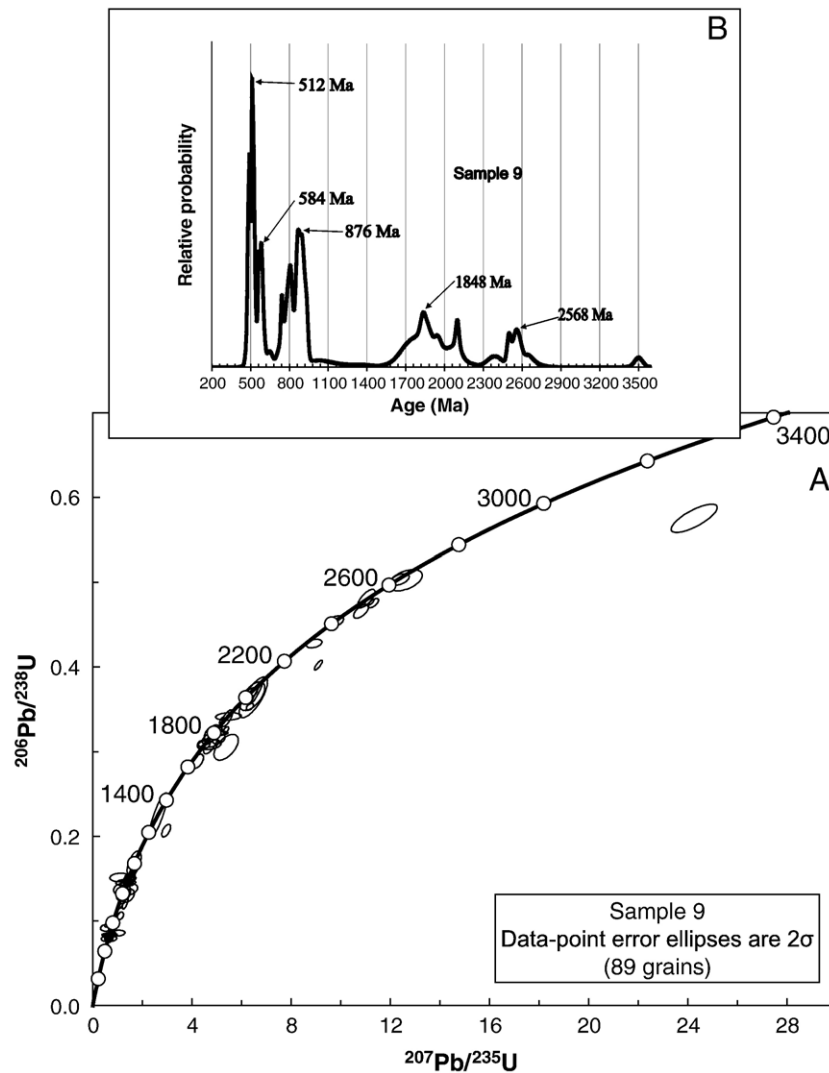

Fig. 13. (A) U–Pb concordia diagram of single detrital-zircon grains for Sample 9 (89 grains total). Error ellipses were at the 2σ level. (B) Relative-age-probability diagram for Sample 9. Note that the relative-age-probability curves show ages and uncertainties (plotted as a normal distribution about the age) from each sample.

presence of the youngest peak at ~504 Ma indicates that the meta-sediments were deposited after the lower Cambrian.

Sample 11 (47° 47.2′N, 107° 21.3′E) was collected from a Silurian to Carboniferous age (Tomurtogoo, 2006) sequence of radiolarian chert, quartzite, and meta-lithic-arkose in southeastern Hentey basin (Fig. 3). The sample was collected from a thin-bedded, meta-lithic-arkose bed that was located ~20 m from the chert bed where Kurihara et al. (2006) discovered Lower Devonian radiolarian. A total of 95 zircon grains were analyzed for this sample and the ages range from ~310 Ma to 881 Ma, mostly clustering around the peak at 340 Ma (Fig. 15A,B). This sample contained seven pre-Devonian zircon grains, one of which was Silurian age (440 Ma), one of which was Ordovician age and five that were Neoproterozoic in age. The 340-Ma peak age of zircon grains suggest the deposition of the meta-sediments occurred after the earliest Carboniferous.

Sample 12 (47° 47.2′N, 107° 21.8′E) was collected from a sequence of Silurian to Carboniferous age (Tomurtogoo, 2006) beds of radiolarian chert, quartzite, meta-pelite and meta-lithic-

arkose in southeastern Hentey basin (Fig. 3). This sample was located ~500 m east of Sample 11 and was 25 m from a chert bed where Kurihara et al. (2006) discovered Upper Silurian conodonts. A total of 98 zircon grains were analyzed for this sample and the ages range from ~317 Ma to 875 Ma, mostly clustering around the peak at 339 Ma (Fig. 16A,B). This sample contained seven pre-Devonian zircon grains, one of which was Ordovician age (480 Ma), two of which were Cambrian age and four of which were Neoproterozoic in age. The 339-Ma peak age of zircon grains suggest the deposition of the rocks occurred after the earliest Carboniferous.

Sample 13 (47° 44.5′N, 106° 19.1′E) was collected from a Silurian to Carboniferous age (Tomurtogoo, 2006) meta-lithic-arkose and meta-pelite sequence in the southern Hentey basin (Fig. 3), which mostly consists of thinly bedded turbidite deposits. A total of 96 zircon grains were analyzed for this sample and the ages range from ~330 Ma to 919 Ma, mostly clustering around the peak at 354 Ma (Fig. 17A,B). This sample contained five pre-Devonian zircon grains, one of which was Silurian age and four grains were Neoproterozoic age. The

Fig. 14. (A) U–Pb concordia diagram of single detrital-zircon grains for Sample 10 (97 grains total). Error ellipses were at the 2σ level. (B) Relative-age-probability diagram for Sample 10. Note that the relative-age-probability curves show ages and uncertainties (plotted as a normal distribution about the age) from each sample.
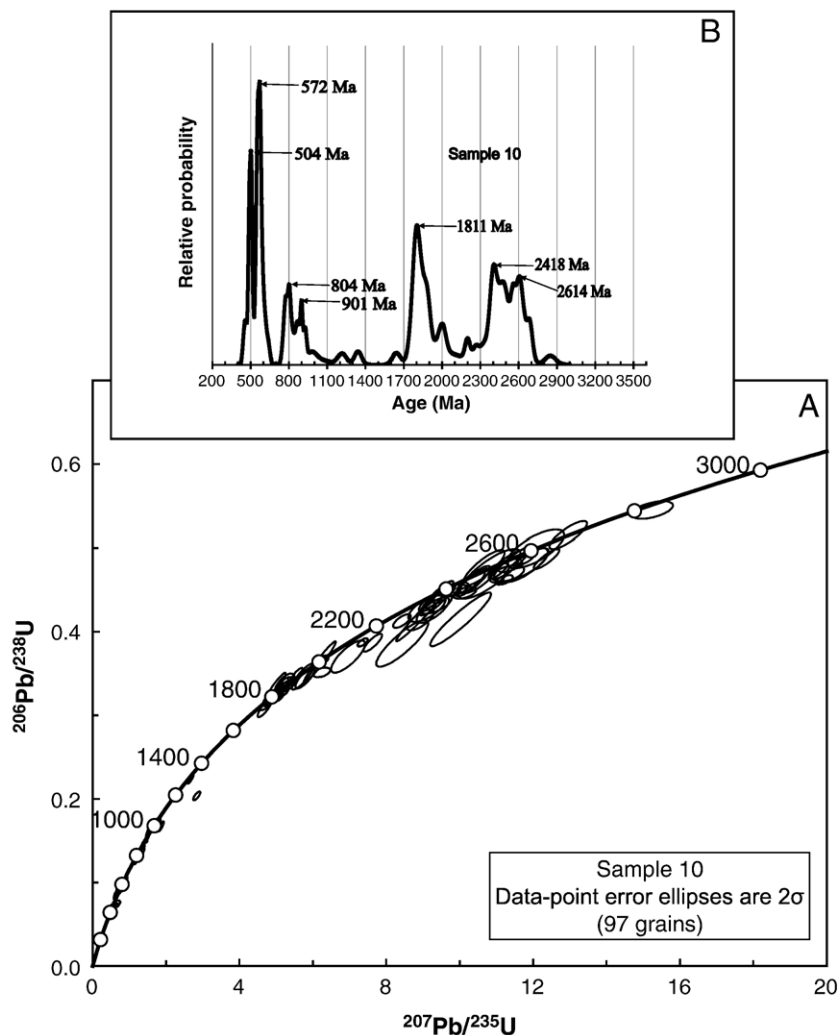
Fig. 15. (A) U–Pb concordia diagram of single detrital-zircon grains for Sample 11 (95 grains total). Error ellipses were at the 2σ level. (B) Relative-age-probability diagram for Sample 11. Note that the relative-age-probability curves show ages and uncertainties (plotted as a normal distribution about the age) from each sample.
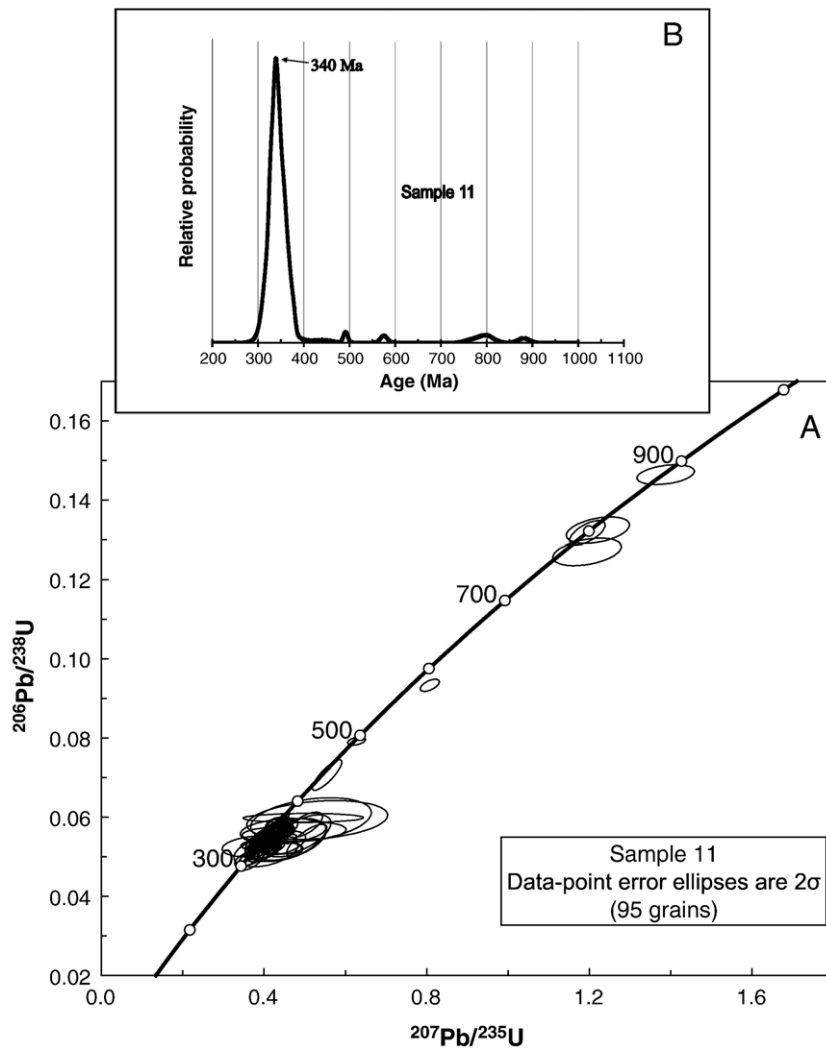
354-Ma peak age of zircon grains suggest the deposition of the meta-sediments occurred after the earliest Carboniferous.

4. Discussion

4.1. Age of the sedimentary rocks

The ages determined from the detrital-zircon samples provide new age constraints for the major sedimentary rocks in the Hentey basin. Using the tectonostratigraphic terrane map of Badarch et al. (2002) as a framework, Tomurtogoo (2006) has defined the ages of tectonostratigraphic units within the Hangay–Hentey "turbidite basin." The most widely distributed of these units has a depositional age that spans from the Silurian to the Carboniferous (Tomurtogoo, 2006). Samples 1–6 and 11–13 were collected from this unit. The peak age from the relative-age-probability diagrams (Figs. 5B, 6B, 7B, 8B, 9B, 10B and Figs. 15B, 16B, 17B) indicated these sediments must be younger than the earliest Carboniferous (339 Ma to 354 Ma). One sample was collected in the Hangay basin (Sample 7) and revealed a similar Carboniferous peak age to Samples 1–6 and 11–13 in the Hentey basin (∼354 Ma) (Fig. 11B). However, unlike the

Hentey basin samples, Sample 7 includes a minor peak age of Silurian (∼435 Ma) (Fig. 11B). The zircon grains that comprise this minor peak may have been derived from igneous rocks that formed in north and central Mongolia during the Ordovician to Silurian (∼450 Ma) (Wickham et al., 1995). Kurimoto and Tungalag (1998) reported K–Ar dates of 453±9.1 Ma within the metamorphic rocks of the Dzag Zone, which was located along the southwest edge of the Hangay basin. It is possible that the Silurian zircon grains may be from the Dzag Zone. From the regional tectonic setting, arc magmatism was active on both sides of the Hangay–Hentey basin during the Devonian and Carboniferous (Wickham et al., 1995; Zorin, 1999; Badarch et al., 2002) (Fig. 3). If zircons were generated by the magmatic arcs and were transported instantaneously to the basin, then the age of the youngest zircons can approximate the age of deposition. This would imply that the meta-sedimentary units from which our samples were collected were all Carboniferous and deposited over 15 Ma span from ∼339 Ma to 354 Ma.

Samples 8–10 provide time constraints for the sedimentary rocks in the northwest part of the Hentey basin (Fig. 3) and were collected from the Haraa terrane (Badarch et al., 2002). The oldest rocks within the Haraa terrane were greenschist
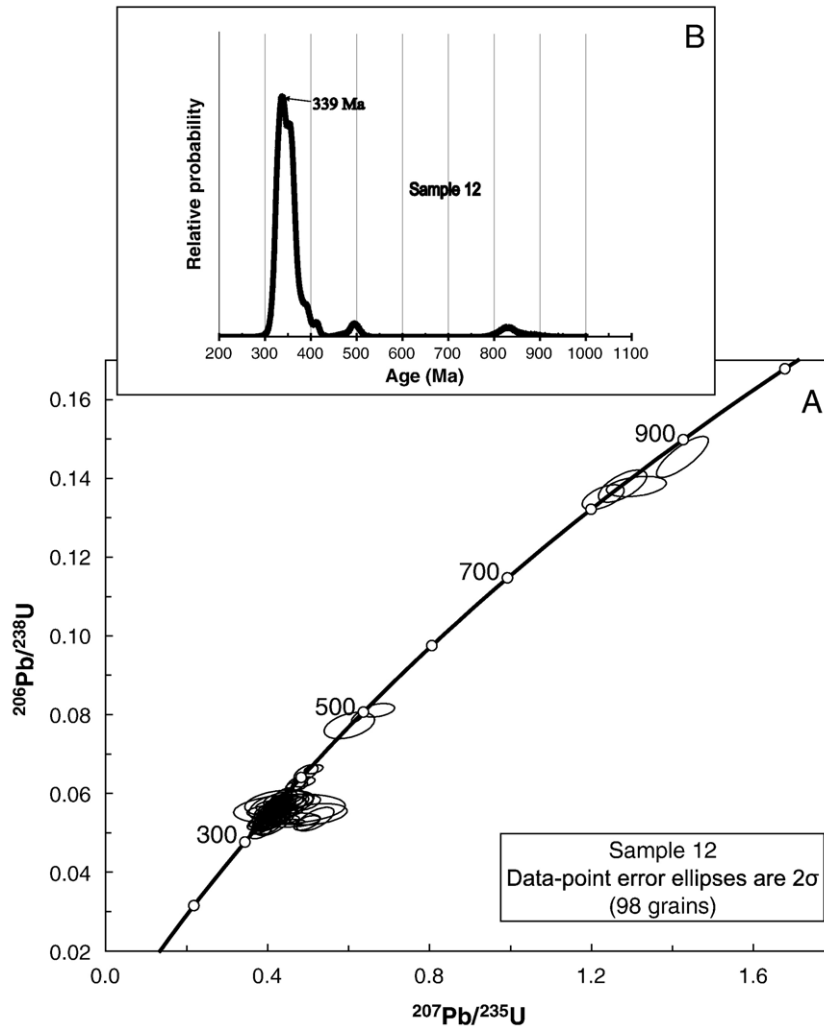
Fig. 16. (A) U–Pb concordia diagram of single detrital-zircon grains for Sample 12 (98 grains total). Error ellipses were at the 2σ level. (B) Relative-age-probability diagram for Sample 12. Note that the relative-age-probability curves show ages and uncertainties (plotted as a normal distribution about the age) from each sample.

metamorphosed sediments of Cambrian age (Badarch et al., 2002). Tomurtogoo (2006) divides the Haraa terrane into two turbidite basins. Tomurtogoo (2006) assigned the northern basin to the Cambrian to Ordovician and the southern basin to the Ordovician to Silurian. Sample 8 was within a Cambrian to Ordovician turbidite basin and reveals a maximum depositional age for these sediments of Neoproterozoic (605 Ma) (Fig. 12B). Samples 9 and 10 were from Tomurtogoo's (2006) Ordovician to Silurian turbidite basin and indicated a maximum depositional age of Cambrian (504 Ma and 512 Ma, respectively) (Figs. 13B and 14B).

4.2. Spatial and temporal variation of detrital-zircon ages

From the age distribution of the detrital-zircon grains, samples were divided into two groups. The first group includes Samples 1–7 and 11–13, all of which show age peaks at 339–354 Ma with less prevalent zircon grains with ages in the 550–400 Ma and 900–700 Ma ranges (Figs. 5B, 6B, 7B, 8B, 9B, 10B, 11B and 15B, 16B, 17B). These samples have depositional ages younger than the earliest Carboniferous. Samples in the

first group were widely distributed across the whole Hentey basin and one sample is from the easternmost part of the Hangay basin. The second group includes Samples 8, 9 and 10. These samples were from units deposited after the start of the Cambrian (Sample 9 and 10; Figs. 13B and 14B, respectively) and Neoproterozoic (Sample 8, Fig. 12B). Samples from the second group were located along the northern edge of the Hangay–Hentey basin (within the Haraa terrane). Samples 8, 9, and 10 also have minor peak ages of Neoproterozoic (804 Ma, 876 Ma and 901 Ma), Paleoproterozoic (1811 Ma, 1848 Ma, 1935 Ma and 2418 Ma), and Archean (2568 Ma and 261 Ma) (Figs. 12B, 13B, and 14B). These Proterozoic and Archean age data indicated that a likely source for these zircon grains may have been the Tuva–Mongol massif, which was located directly north of the sample localities (Fig. 3). However, Salnikova et al. (2001) pointed out that the protolith for the metamorphic rocks of the Tuva–Mongol massif was early Paleozoic and may not have been Proterozoic to Archean. If the Tuva–Mongol massif was not the source for the Precambrian zircon grains discovered in Samples 8, 9 and 10, they may have been derived from the Siberian craton, which contains remnants of many magmatic
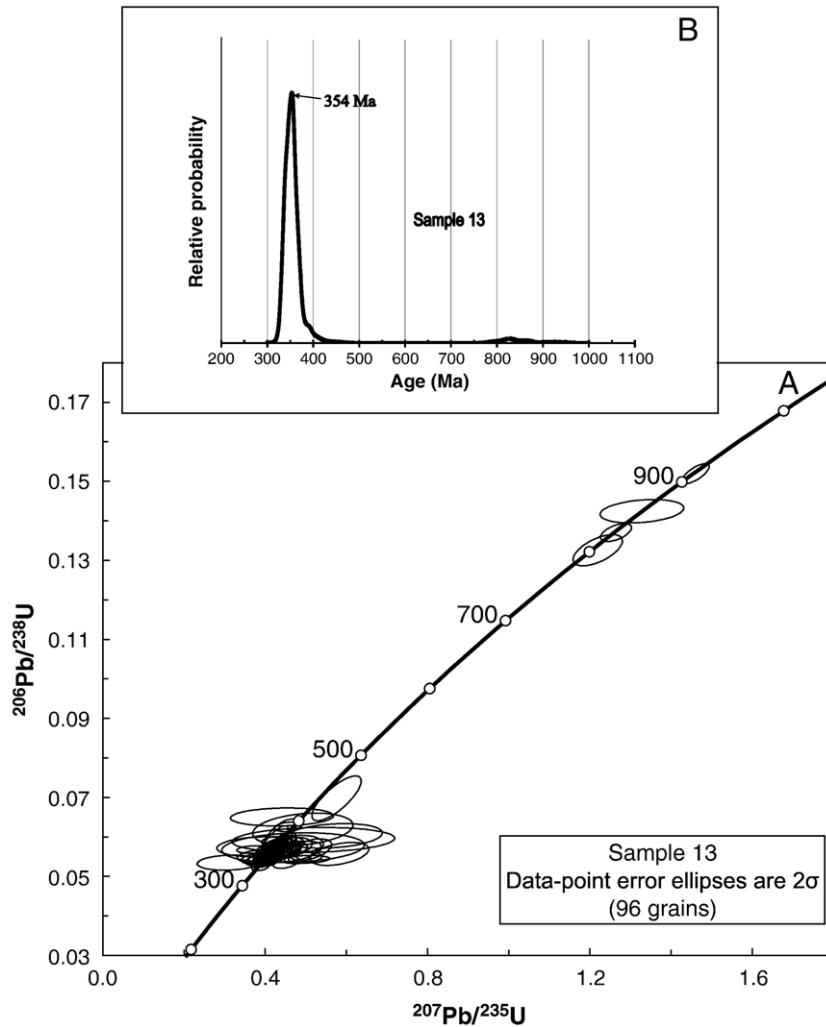
Fig. 17. (A) U–Pb concordia diagram of single detrital-zircon grains for Sample 13 (96 grains total). Error ellipses were at the 2σ level. (B) Relative-age-probability diagram for Sample 13. Note that the relative-age-probability curves show ages and uncertainties (plotted as a normal distribution about the age) from each sample.

events of Proterozoic and Archean age (e.g., Zonenshain et al., 1990; Poller et al., 2005; Rojas-Agramonte et al., 2006).

At least two end-member interpretations for the zircon age distribution will be proposed. First, the change in age distribution between the two groups represents a temporal variation of provenance. That is, all the samples were sourced from the same geographic region or basement rocks with same age distributions, but later geologic processes caused complete coverage of the older source terranes and exposure of younger zircon grains. In the context of the Sengör and Natal'in (1996) model, this would imply that basement rocks with similar age distributions were the sources for both the southern and northern margins of the Hangay–Hentey basin. We consider this interpretation highly unlikely, because the older zircons would be recycled into younger sedimentary units and thus be detected by our analysis. If one or two samples missed the Middle Proterozoic to Archean zircon grains, they would be explained by the samples being located in small drainage basins receiving a local point source. However, because the samples cover a large region of the basin, it was highly unlikely that the Proterozoic and Archean zircon grains were missed.

The second possibility was that the differences in age spectra between the two groups resulted from different source terranes that supplied detrital-zircon grains with different ages. Specifically, the samples from the southern part of the basin had a source from a magmatic arc in the south that has a 550–400 Ma and 900–700 Ma basement, whereas samples from the northern part of the basin had a source from the north that has a 600–500 Ma magmatic arc rocks overlying Proterozoic and Archean rocks (Tuva–Mongol massif or Siberian craton). This interpretation may be problematical given that Samples 3 and 4 were located along the northern margin of the basin. Samples 3 and 4 have age distributions similar to those located in the southern part of the basin (e.g., Samples 1, 2, 5, 6, 11, 12, and 13). Two possible explanations for this was that Samples 3 and 4 have been displaced along a northeast-striking, right-lateral strike-slip fault. Another possible interpretation was the Haraa terrane in which Samples 8, 9 and 10 were collected was displaced by a large north-dipping thrust, placing the northerly-sourced rocks in the hanging wall and the southerly-sourced rocks (Samples 1–7 and 11–13) in the footwall. In the context of this interpretation, Samples 3 and 4 are located in a thrust window. Byamba (1990)

South　　　　　　　　　　　　　　　　　　　　　　　　　　　　North

Samples 1, 2, 5, 6, 11, 12, and 13
Samples 3?, 4?

Samples 8, 9 and 10

Hentey basin

Fore-arc basin　　　　　**accretionary wedge**

Southern Mongolian
arc (354-339 Ma)
with a 900-700 Ma
crystalline basement

? ?

Tuva-Mongol massif or Siberian
basement with 900 to 800 Ma and
1.8 to 2.5 Ga crystalline rocks.

600-500 Ma arc rocks
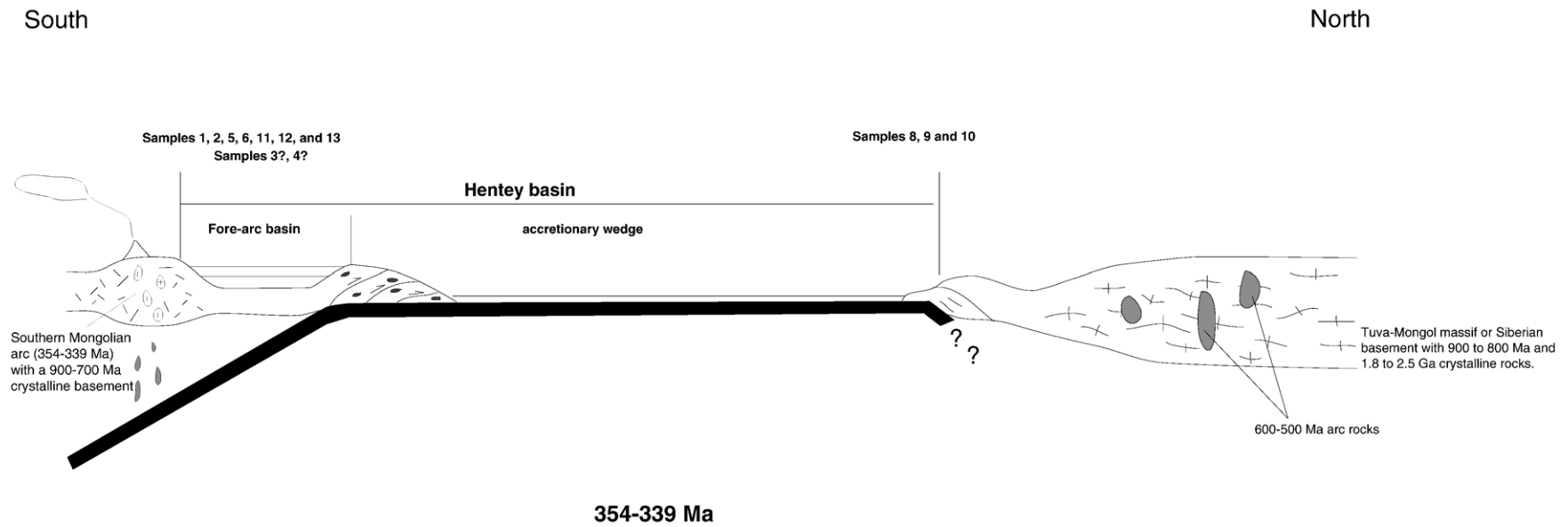
354-339 Ma

Fig. 18. A tectonic model for the Hentey basin (Mongol–Okhotsk Ocean) from 354 to 339 Ma. Detrital-zircon grains for the Hangay–Hentey basin may have been derived from the Southern Mongolian arc (Samples 1 through 6 and 11 through 13). Detrital-zircon grains from Samples 8 through 10 indicate that the source area may have been the Tuva–Mongol massif and/or the Siberian craton.

has shown that the location of Samples 3 and 4 was part of a fault block that was structurally separated from the location of Samples 8, 9 and 10 (Haraa terrane). Detailed structural mapping between the units represented by Samples 3 and 4 and the Haraa terrane is required in the future to test these interpretations.

We favor the second interpretation in which Samples 3 and 4 were deposited in a similar tectonic setting as Samples 1, 2, 5, 6, 11, 12, and 13. The spectra of ages for the detrital-zircon grains for these samples were similar (Figs. 5B, 6B, 7B, 8B, 9B, 10B, 11B and Figs. 15B, 16B, 17B). Fig. 18 illustrates the tectonic model that explains the detrital-zircon age results from our study. In this model, a fore-arc basin developed next to a south-dipping subduction zone of Carboniferous age. Samples 1–6 and 11–13 were deposited into this basin. Igneous rocks formed during the Carboniferous directly south of the Hangay–Hentey basin and may be the source for the 339–354 Ma zircon grains (Fig. 3). Fig. 18 also indicates the possibility of a north-dipping subduction zone because there were Devonian to Carboniferous volcanic and plutonic rocks located north of the Hentey basin (Fig. 3). It was possible that there may have been a fore-arc basin located along the northern margin of the Hentey basin.

4.3. Questions raised by this study

All the interpretations presented above are highly speculative due to lack of detailed field mapping to define the nature and age of the contacts of the geologic terranes. However, our data provide both new age constraints for the development of the Hangay–Hentey basin and raise several questions.

(1) *What was the tectonic origin of the Hangay–Hentey basin?* According to Sengör and Natal'in model (1996), the basin was a long-lived feature between ~620 Ma and 200 Ma. The basement rocks (Tuva–Mongol massif) on both sides of the Hangay–Hentey basin originated from the Siberia craton. Our results suggest that the provenance for detrital-zircon grains were quite different between the two sides of the basin and imply that the southern basin margin had no geologic connection with the northern basin margin. That is, the inferred Carboniferous arc in our tectonic model (Fig. 18) must have a different paleogeographic origin from Tuva–Mongol/Siberia craton. This raises the question of how the Hangay–Hentey basin was closed.

(2) *What was the structural relationship between units with drastically different detrital-zircon ages?* Was the age difference between the samples due to tectonic juxtaposition or controlled by the arrangement of drainage systems? Addressing this question requires a combination of detailed structural and sedimentologic studies. One such study has been performed where Samples 11 and 12 were collected. This was the same site where Kurihara et al. (2006) discovered Devonian radiolarian and Silurian conodants within chert beds. Samples 11 and 12 have a maximum depositional age of early Carboniferous and were collected from beds directly juxtaposed against Devonian and Silurian chert beds (Figs. 15B and 16B). We interpret that these rocks were juxtaposed in an accretionary wedge.

(3) *When did the Hangay–Hentey basin first begin to evolve?* According to the Sengör and Natal'in (1996) model, the basin should have been in existence since the Neoproterozoic and continued to evolve until the early Mesozoic. The maximum depositional age for Samples 8, 9 and 10 (Haraa terrane) of Cambrian to Neoproterozoic age are evidence for this early deposition into the Khangai–Khantey Ocean, which was the precursor to the Hangay–Hentey basin. However, this interpretation may change as more kinematic and age data from the structures that bound the Haraa terrane are published. It was also possible that the older Neoproterozoic–Silurian strata in the Hangay–Hentey basin were covered by a younger Devonian–Carboniferous flysch sequence.

(4) *When was the Mongol–Okhotsk Ocean finally close?* From the detrital-zircon age data presented in this study, it was known that the Mongol–Okhotsk Ocean was open in the Carboniferous. However, when the ocean closed is disputed. Kravchinsky et al. (2001) proposed closure of the Mongol–Okhotsk Ocean beginning in the Permian and complete closure occurred from the late Jurassic to early Cretaceous. Others support final closure of the ocean in the early to middle Jurassic (Zorin et al., 1993; Didenko et al., 1994), late Jurassic (Jishun and Tingyu, 1989; Nie, 1991) and late Cretaceous (Enkin et al., 1992; Halim et al., 1998). Determining when the basin closed is an important part of the tectonic history and will require more work. Determining when the penetrative deformation formed throughout the basin is essential to understanding when the basin closed.

5. Conclusions

We conducted U–Pb detrital-zircon geochronological investigation across the Hangay–Hentey basin of Mongolia, which was the largest flysch complex in the CAOS. We analyzed 13 samples collected from Neoproterozoic to Paleozoic turbidite units across the basin and our results allow us to reevaluate the age assignment of some of the key geologic units across the basin. In general, the age assignment of many of the meta-sedimentary rocks within the Hangay–Hentey basin was remarkably similar and indicated deposition at or after the early Carboniferous. These samples contained few Proterozoic-to Archean-age zircon grains. Although the number of our samples was quite small, the large spatial coverage of our sampling raises the possibility that the Hangay–Hentey basin did not start to evolve, at least as a flysch basin, until after early Carboniferous. U–Pb detrital-zircon geochronology also allowed us to distinguish a second group of meta-sedimentary rocks that were located in the northern part of the Hangay–Hentey basin. These samples indicated deposition at or after the Cambrian to Neoproterozoic. We explained the age distribution of these rocks by dividing the Hangay–Hentey basin into two tectonic systems. The southern and western part of the basin represents a north-facing fore-arc basin fringing an early Carboniferous arc with a 900–700 Ma basement, whereas the northeastern part of the basin was composed of a large accretionary complex that has an older maximum depositional

age (Cambrian to Neoproterozoic). These meta-sediments were derived from both magmatic arc rocks from 600 to 500 Ma and Proterozoic to Archean age rocks of the Tuva–Mongol massif and/or Siberia craton.

Acknowledgements

Appendix A. Supplementary data

Supplementary data associated with this article can be found, in the online version, at doi:10.1016/j.tecto.2007.11.052.

References

Badarch, G., Cunningham, W.D., Windley, B.F., 2002. A new terrane subdivision for Mongolia: implications for the Phanerozoic crustal growth of Central Asia. J. Asian Earth Sci. 21, 87–110.

Byamba, J., (Editor), 1990. Central and Eastern Mongolian Geological map (scale 1:500,000). Regional Geological Mapping Division, Ulaanbaatar, Mongolia.

Chen, C., Hsu, W., 1995. Magmatism at the onset of back-arc basin spreading in Okinawa Trough. J. Volcanol. Geotherm. Res. 69, 313–322.

Didenko, A.N., Mossakovskii, A.A., Pecherskii, D.M., Ruzhentsev, S.V., Samygin, S.G., Kheraskova, T.N., 1994. Geodynamics of the Central-Asian Paleozoic Oceans. Russ. Geol. Geophys. 35, 48–61.

Dobretsov, N.L., Buslov, M.M., Delvaux, D., Berzin, N.A., Ermikov, V.D., 1996. Meso-and Cenozoic tectonics of the central Asian mountain belt: effects of lithospheric plate interaction and mantle plumes. Int. Geol. Rev. 38, 430–466.

Dorjsuren, B., Tomurtogoo, O., Dejidmaa, G., Mahbadar, T., Bujinlkham, B., 2004. New member of the Altan Ovoo Formation. Mong. Geosci. 26, 53–56.

Enkin, R.J., Yang, Z.Y., Chen, Y., Courtillot, V., 1992. Paleomagnetic constraints on the geodynamic history of China from the Permian to the present. J. Geophys. Res. 97, 13,953–13,989.

Gehrels, G.E., Valencia, V., Pullen, A., 2006. Detrital zircon geochronology by Laser-Ablation Multicollector ICPMS at the Arizona LaserChron Center. In: Loszewski, T., Huff, W. (Eds.), Geochronology: Emerging Opportunities. Paleontology Society Short Course: Paleontology Society Papers, vol. 11, p. 10.

Halim, N., Kravchinsky, V., Gilder, S., Cogne, J.-P., Alexyutin, M., Sorokin, A., Courtillot, V., Chen, Y., 1998. A paleomagnetic study from the Mongol–Okhotsk region: rotated Early Cretaceous volcanics and remagnetized Mesozoic sediments. Earth Planet. Sci. Lett. 159, 133–145.

Hsu, K.J., Chen, H., 1999. Geologic Atlas of China: An Application of the Tectonic Facies Concepts to the Geology of China. New York, Elsevier.

Jahn, B., Capdevila, R., Liu, D., Vernon, A., Badarch, G., 2004. Sources of Phanerozoic granitoids in the transect Bayanhongor–Ulaan Baatar, Mongolia: geochemical and Nd isotopic evidence and implications for Phanerozoic crustal growth. J. Asian Earth Sci. 23, 629–653.

Jishun, R., Tingyu, C., 1989. Tectonic evolution of the continental lithosphere in eastern China and adjacent areas. J. Southeast Asian Earth Sci. 3, 17–27.

Kovelenko, V.I., Yarmolyuk, V.V., Kovach, V.P., Kotov, A.B., Kozakov, I.K., Salnikova, E.B., Larin, A.M., 2004. Isotopic provinces, mechanism of generation and sources of the continental crust in the Central Asian mobile belt: geologic and isotopic evidence. J. Asian Earth Sci. 23, 605–627.

Kravchinsky, V.A., Konstantinov, K.M., Cogne, J.-P., 2001. Palaeomagnetic study of Vendian and Early Cambrian rocks of South Siberia and Central Mongolia: was the Siberian platform assembled at this time? Precambrian Res. 110, 61–92.

Kurihara, T., Tsukada, K., Otoh, S., Kashiwagi, K., Minjin, C., Sersmaa, G., Dorjsuren, B., Bujinlkham, B., 2006. Middle Paleozoic radiolarians from the Gorkhi Formation, central Mongolia. In: Tomurhuu, D., Natal'in, B., Ya, A., Khishigsuren, S., Erdenesaikhan, G. (Eds.), Structural and tectonic correlation across the Central Asian Orogenic Collage: implications for continental growth and intracontinental deformation. Abstract and Guidebook Volume, Workshop IGCP-480. Mongolian University of Science and Technology Press, Ulaanbaatar, p. 67.

Kurimoto, C., Tungalag, F., 1998. K–Ar ages of white micas from pelitic schists of the Bayankhongor area, west Mongolia. Bull. Geol. Surv. Jap. 49, 19–23.

Ludwig, K.R., 2003. Isoplot 3.00. Berkeley Geochronology Center, Special Publication No. 4.

Mossakovsky, A.A., Ruzhentsev, S.V., Samygin, S.G., Kheraskova, T.N., 1994. Central Asian Fold Belt: geodynamic evolution and formation history. Geotech. 27, 445–474.

Nie, S., Rowley, D.B., Ziegler, A.M., 1990. Constraints on the locations of Asian microcontinents. In: McKerrow, W.S., Scotese, C.R. (Eds.), Paleo-Tethys during the late Paleozoic, in Paleozoic Paleogeography and Biogeography. Mem. Geol. Soc. Lon., pp. 397–408.

Nie, S., 1991. Paleoclimatic and paleomagnetic constraints on the Paleozoic Reconstructions of south China, north China and Tarim. Tectonophysics 196, 279–308.

Poller, U., Gladkochub, D., Donskaya, T., Mazukabzov, A., Sklyarov, E., Todt, W., 2005. Multistage magmatic and metamorphic evolution in the Southern Siberian Craton: Archean and Palaeoproterozoic zircon ages revealed by SRIMP and TIMS. Precambrian Res. 136, 353–368.

Rojas-Agramonte, Y., Kröner, A., Badarch, G., Liu, D.Y., Condie, K.C., Donskaya, T., Demoux, A., Wingate, M.T.D., 2006. Detrital and xenocrystic zircon ages in the Central Asian Orogenic Belt of Mongolia: comparison with the Siberian craton and Gondwana. In: Tomurhuu, D., Natal'in, B., Ya, A., Khishigsuren, S., Erdenesaikhan, G. (Eds.), Structural and tectonic correlation across the Central Asian Orogenic Collage: implications for continental growth and intracontinental deformation. Abstract and Guidebook Volume, Workshop IGCP-480. Mongolian University of Science and Technology Press, Ulaanbaatar, pp. 58–59.

Salnikova, E.B., Kozakov, I.K., Kotov, A., Kröner, A., Todt, W., Bibikova, E.V., Nutman, A., Yakovleva, S.Z., Kovach, V.P., 2001. Age of Palaeozoic granites and metamorphism in the Tuvino–Mongolian Massif of the Central Asian Mobile Belt: loss of a Precambrian microcontinent. Precambrian Res. 110, 143–164.

Sengör, A.M.C., Natal'in, B.A., Burtman, V.S., 1993. Evolution of the Altaid tectonic collage and Paleozoic crustal growth in Eurasia. Nature 364, 299–307.

Sengör, A.M.C., Natal'in, B.A., 1996. Paleotectonics of Asia: fragments of a synthesis In: Yin, A., Harrison, T.M. (Eds.), The Tectonics of Asia. Cambridge Univ. Press, New York, pp. 486–640.

Stacey, J.S., Kramers, J.D., 1975. Approximation of terrestrial lead isotope evolution by a two-stage model. Earth Planet. Sci. Lett. 26, 207–221.

Tomurtogoo, O., 2006. Tectonic framework of Mongolia. In: Tomurhuu, D., Natal'in, B., Ya, A., Khishigsuren, S., Erdenesaikhan, G. (Eds.), Structural and tectonic correlation across the Central Asian Orogenic Collage: implications for continental growth and intracontinental deformation. Abstract and Guidebook Volume, Workshop IGCP-480. Mongolian University of Science and Technology Press, Ulaanbaatar, pp. 18–20.

Wickham, S.M., Litvinovsky, B.A., Zanvilevich, A.N., Bindeman, I.N., 1995. Geochemical evolution of Phanerozoic magmatism in Transbaikalia, East Asia: a key constraint on the origin of K-rich silicic magmas and the process of cratonization. J. Geophys. Res. 100, 15,641–15,654.

Windley, B.F., Alexeiev, D., Xiao, W., Kröner, A., Badarch, G., 2007. Tectonic model for accretion of the Central Asian Orogenic Belt. J. Geol. Soc. (Lond.) 164, 31–47.

Xiao, W., Windley, B.F., Hao, J., Zhai, M., 2003. Accretion leading to collision and the Permian Solonker suture, Inner Mongolia, China: termination of Central Asian Orogenic Belt. Tectonics 22, 1069. doi:10.1029/2002TC001484.

Xiao, W., Windley, B.F., Badarch, G., Sun, S., Li, J., Qin, K., Wang, Z., 2004a. Palaeozoic accretionary and convergent tectonics of the southern Altaids: implications for the growth of Central Asia. J. Geol. Soc. (Lond.) 161, 339–342.

Xiao, W., Zhang, L.-C., Qin, K.-Z., Sun, S., Li, J., 2004b. Paleozoic accretionary and collisional tectonics of the eastern Tienshan (China): implications for the continental growth of Central Asia. Am. J. Sci. 304, 370–395.

Yin, A., Nie, S., 1993. An indention model for North and South China collision and the development of the Tan Lu and Honam fault systems, eastern Asia. Tectonics 12, 801–813.

Yin, A., Nie, S., 1996. A Phanerozoic palinspastic reconstruction of China and its neighboring regions. In: Yin, A., Harrison, T.M. (Eds.), The Tectonics of Asia. Cambridge Univ. Press, New York, pp. 442–485.

Zonenshain, L.P., Kusmin, M.I., Natapov, L.M., 1990. Mongol-Okhotsk Foldbelt. In: Page, B.M. (Ed.), Geology of the USSR: a plate-tectonic synthesis. Geody. Ser. 21 Am. Geophy. Un, Washington, D.C.

Zorin, Y.A., Belichenko, V.G., Turutanov, E.K., Kozhevnikov, V.M., Ruzhent-sev, S.V., Dergunov, A.B., Filippova, I.B., Tomurtogoo, O., Arvisbaatar, N., Bayasgalan, T., Biambaa, C., Khosbayar, P., 1993. The South Siberia–Central Mongolian transect. Tectonophysics 225, 361–378.

Zorin, Y.A., 1999. Geodynamics of the western part of the Mongolia–Okhotsk collisional belt, Trans-Baikal region (Russia) and Mongolia. Tectonophysics 306, 33–56.